USGS-OFR-92-245

U.S. DEPARTMENT OF THE INTERIOR
U.S. GEOLOGICAL SURVEY

WIDE-ANGLE SEISMIC RECORDINGS OBTAINED DURING SEISMIC REFLECTION PROFILING BY THE S.P. LEE OFFSHORE THE LOMA PRIETA EPICENTER

By

Thomas M. Brocher[1], Michael J. Moses[1], and Stephen D. Lewis[2]

Open-File Report 92-245

[1]345 Middlefield Road, M/S 977, Menlo Park, CA 94025
[2]345 Middlefield Road, M/S 999, Menlo Park, CA 94025

Menlo Park, California
1992

CONTENTS

FIGURES

FIGURES CONTINUED

TABLES

ABSTRACT

The U.S. Geological Survey deployed two temporary onshore arrays of seismic recorders transverse to and straddling the San Andreas fault at the latitude of Loma Prieta during marine seismic reflection profiling of the north-central California margin conducted in May 1990. The marine reflection profiles were acquired for the Offshore Geological Framework Program using the R/V **S.P. Lee**, which towed a ten-element, 40 liter (2424 cu. in.) airgun array. Nineteen three-component land stations continuously recorded the airgun signals produced by the reflection profiling at large offsets. This report describes the experiment, provides the locations and times of operation of all the recorders, presents the data reduction scheme followed, and provides examples of the recorded wide-angle seismic data.

INTRODUCTION AND OBJECTIVES

Knowledge of the structure of the mid- to lower-crust offshore central California is fundamental to the understanding of the tectonic processes associated with, and earthquake hazards posed by, ongoing transpression. Since early studies of the continental margin off California (Uchipi and Emery, 1963; Curray, 1966), workers have recognized that accretionary tectonics during the Mesozoic created a typical trench and arc geometry offshore central California which has been disrupted by Cenozoic transtension and subsequent transpression (e.g., Dickinson, 1970; Ernst, 1971; Saleeby, 1986; McCulloch, 1987). Major anticlinal fold structures in the offshore Santa Maria basin have been dated at 3 to 5 m.y., suggesting that ongoing compressional forces related to Pacific plate motion changes may have begun at that time (McCulloch, 1987; Clark and others, 1991). Active transpression across the margin has been inferred from geodetic, focal mechanism, stress measurements, and other data (Zoback and others, 1987). The ongoing transpressional tectonics requires subhorizontal detachment surfaces to accommodate both the compressional and strike-slip motion (Namson and Davis, 1988), but the geometry of these surfaces in north-central California, and their relation to the San Andreas fault, is currently not well

known. In the vicinity of Morro Bay, south of Monterey, seismic reflection/refraction profiling by the Pacific Gas and Electric Company and EDGE (a consortium of university investigators) suggests that the outer margin and shelf are underlain at mid-crustal levels by oceanic crust of the Farallon Plate, and that the top of the oceanic crust may act or have acted as a subhorizontal detachment surface (Ewing and Talwani, 1991).

The Loma Prieta magnitude 7.1 earthquake of October 17, 1989 served both as a reminder of the active transpression occurring along the San Andreas fault and as a catalyst for framework studies aimed at better understanding the crustal structure in its vicinity (U.S. Geological Survey Staff, 1990). Large amplitude reflections from the mid- to lower-crust and upper mantle may have increased ground motions produced by the earthquake at some distant sites (Somerville and Yoshimura, 1990), and provide additional motivation for the delineation of subhorizontal structures in the mid- to lower-crust. In the following we report the primary data resulting from an onshore-offshore seismic reflection/refraction investigation of the crustal structure of the California continental margin in the vicinity of the Loma Prieta earthquake.

DATA ACQUISITION AND PROCESSING

In May, 1990, the U.S. Geological Survey (USGS) conducted a marine seismic reflection investigation of the central California margin (Lewis, 1990; fig. 1a). The airgun array used for reflection profiling also served as a sound source for onshore seismic recorders positioned across the epicentral region of the Loma Prieta earthquake. The 10-element airgun array towed by the R/V **S.P. Lee** totalled 40 liters (2424 cu. in.) and generated seismic signals for two temporary onshore seismic recorder arrays deployed transverse to and straddling the San Andreas fault at the latitude of Loma Prieta and Saratoga (fig. 1b). The main recorder array, across Loma Prieta, consisted of 13 stations stretching from the coast landward some 92 km. A shorter array, located 25 km northeast of Loma Prieta, consisted of 6 stations stretching landward about 70 km from Ano Nuevo (Table 1). These arrays were used to record two 61-km-long, colinear, off-end, reflection

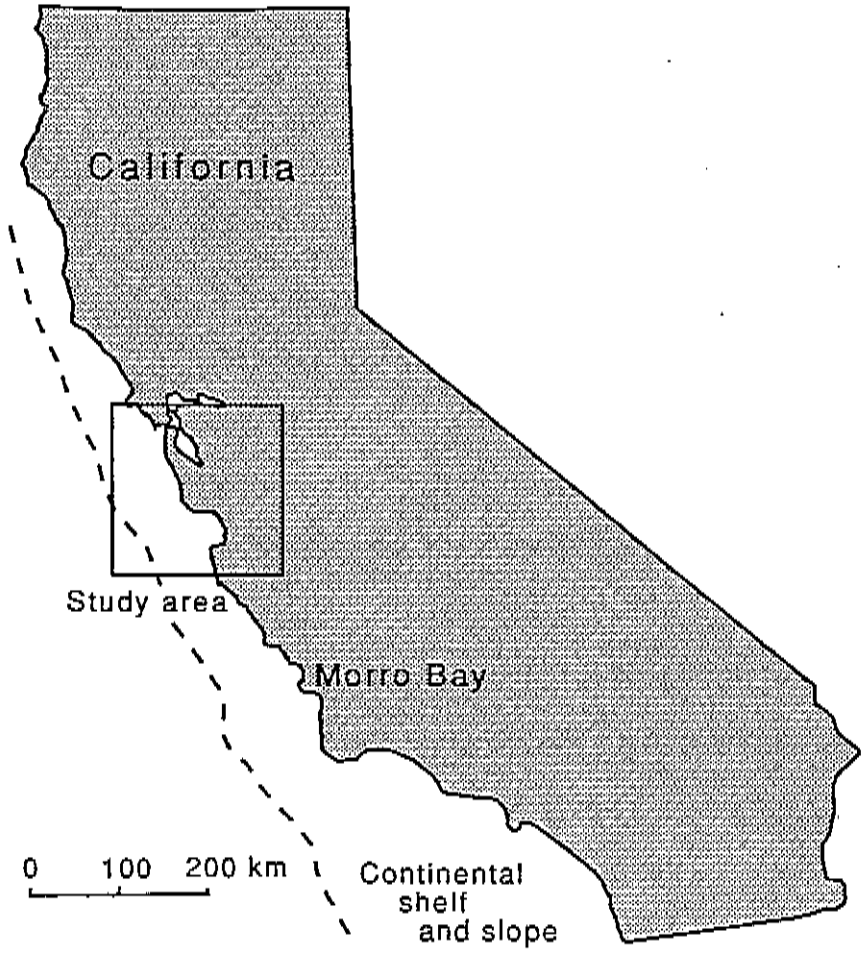

FIGURE 1. (A) Location map of California showing the study area and position of the base of the continental slope.

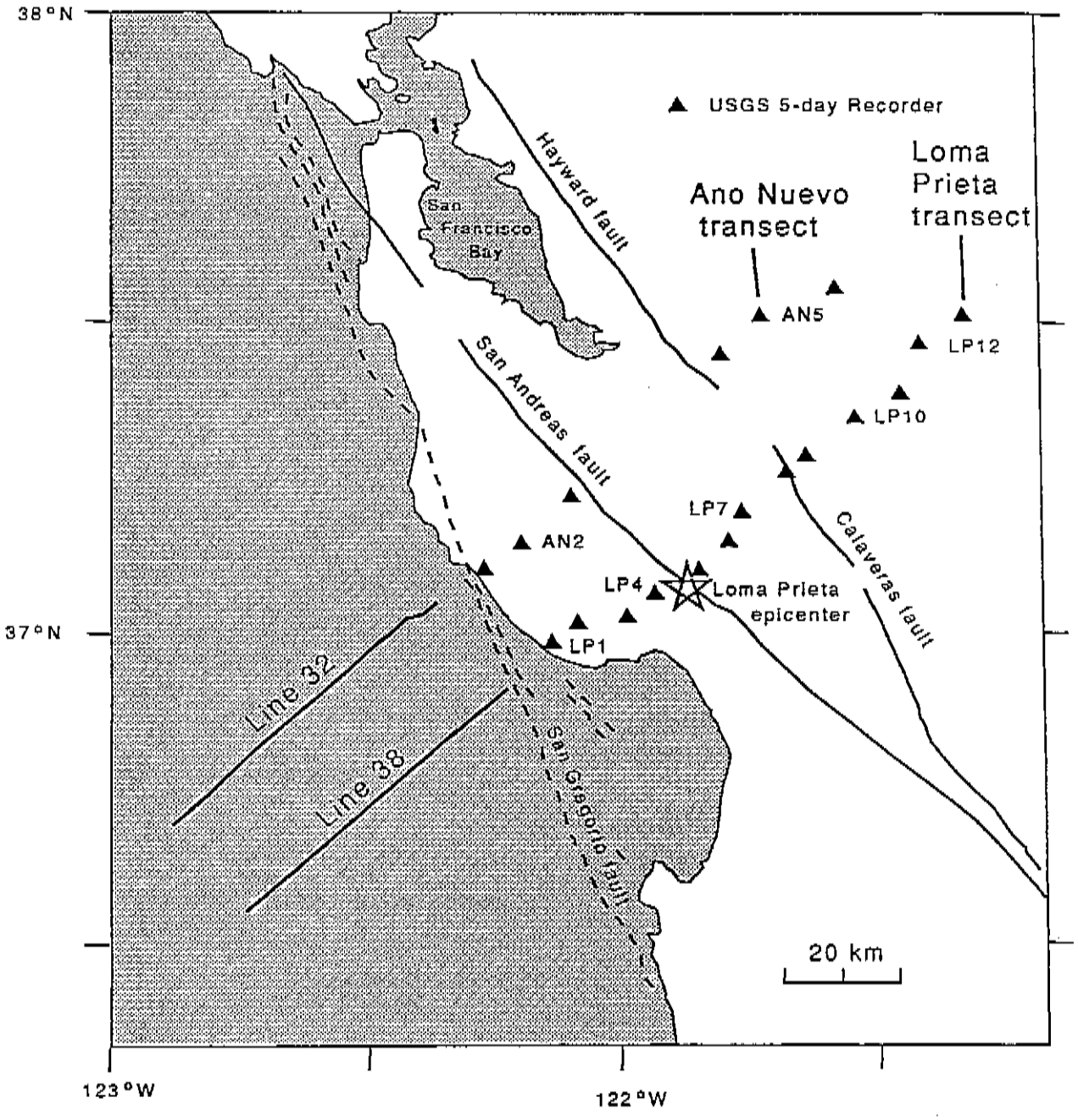

FIGURE 1. (B) Map of central California showing the locations of the marine reflection lines 32 and 38, temporary seismic recorders (filled triangles), and selected faults. The epicenter of the 17 Oct. 1989 magnitude 7.1 earthquake at Loma Prieta is shown as a star.

TABLE 1. 5-day Recorder Locations and Elevations

Site No.	Name	Latitude (N) Deg. Min.	Longitude (W) Deg. Min.	Elevation (m)
LP-1*	Majors Creek	36 59.39568	122 08.03406	170
LP-2	Empire Grade	37 01.41960	122 05.10222	364
LP-3	Happy Valley	37 01.74468	121 59.16768	74
LP-4	Olive Springs	37 04.12782	121 55.63542	240
LP-5	Loma Prieta	37 06.48384	121 50.55318	1081
LP-6	Casa Loma Rd.	37 09.09006	121 46.94538	246
LP-7	Bailey Rd.	37 11.93616	121 45.54030	113
LP-8	Coe Ranch	37 15.54252	121 40.30656	370
LP-9*	San Felipe Rch.	37 17.32848	121 38.03904	860
LP-10	Arnold Ranch	37 20.89050	121 32.02650	663
LP-11*	Red Mtn.	37 23.25432	121 26.85060	763
LP-12	Arkansas Cyn.	37 27.99576	121 24.45276	950
LP-13	Ingram Cyn.	37 30.64266	121 19.27704	235
AN-1	Waddell Creek	37 06.41322	122 15.87570	283
AN-2*	Eagle Creek	37 08.86650	122 11.63766	753
AN-3	Mt. Bielawski	37 13.35756	122 05.60364	987
AN-4	Calaveras Res.	37 27.00354	121 47.80038	270
AN-5	Valpe Ridge	37 30.79374	121 43.03188	1073
AN-6	Mines Road	37 33.32334	121 34.40016	618

*Stations LP-1, LP-9, LP-11, and AN-2 consisted of a transmitter broadcasting signals from a vertical seismometer only.

lines (32 and 38; fig. 1b) as well as several shorter lines having a fan geometry to the near linear receiver arrays. The goals of the wide-angle recording were to place constraints on the mid- to lower-crustal structure in the vicinity of the epicenter of the 1989 Loma Prieta earthquake, and to look at variations in this structure along the strike of the San Andreas fault.

The wide-angle data were recorded using analog three-component, five-day seismic recorders described by Criley and Eaton (1978). Although many of the field procedures used to deploy the five-day recorders were identical to those described for a similar experiment in southern

Alaska (Brocher and Moses, 1990), the simpler logistics of north-central California allowed minor changes in the field method (Appendix). For our study, the five-day recorders were deployed along access roads and were turned on prior to the acquisition of the marine reflection lines. At four sites (LP-1, 9, 11 and AN-2), seismic signals from only a vertical-component seismometer were telemetered to an adjacent five-day recorder for recording.

The internal clock of the five-day recorders was calibrated by WWVB radio signals recorded by each receiver. Comparison of the internal clock and WWVB signals allowed us to accurately determine and remove the drift of the internal clock (see Brocher and Moses, 1990). As a check on the absolute timing provided by WWVB, signals from a OMEGA clock receiver, accurate to within a millisecond after correction for path delays, were recorded for more than 5 minutes at the beginning of each recorder tape.

The calculation of airgun array shot times from "start of recording cycle" times on the R/V **S.P. Lee**, the GPS positioning of the receivers, and navigation of the airgun shot locations is described in the Appendix. For each receiver, we generated computer files containing shot times and ranges for each seismic reflection line.

The playback and digitization of the five-day tapes, the formating of the digitized data into SEG-Y format, and the subsequent processing of the record sections is described in the Appendix. The Appendix also reviews procedures that were introduced during this experiment. The Appendix also briefly describes the SEG-Y format in which the tapes were written. Record sections reduced using a velocity of 6 km/s were generated by this procedure. Deconvolution of the data acquired near Loma Prieta tended to be less successful than that for data acquired in the northern Gulf of Alaska (Brocher and Moses, 1990), primarily because of the lower signal-to-noise levels observed in this study.

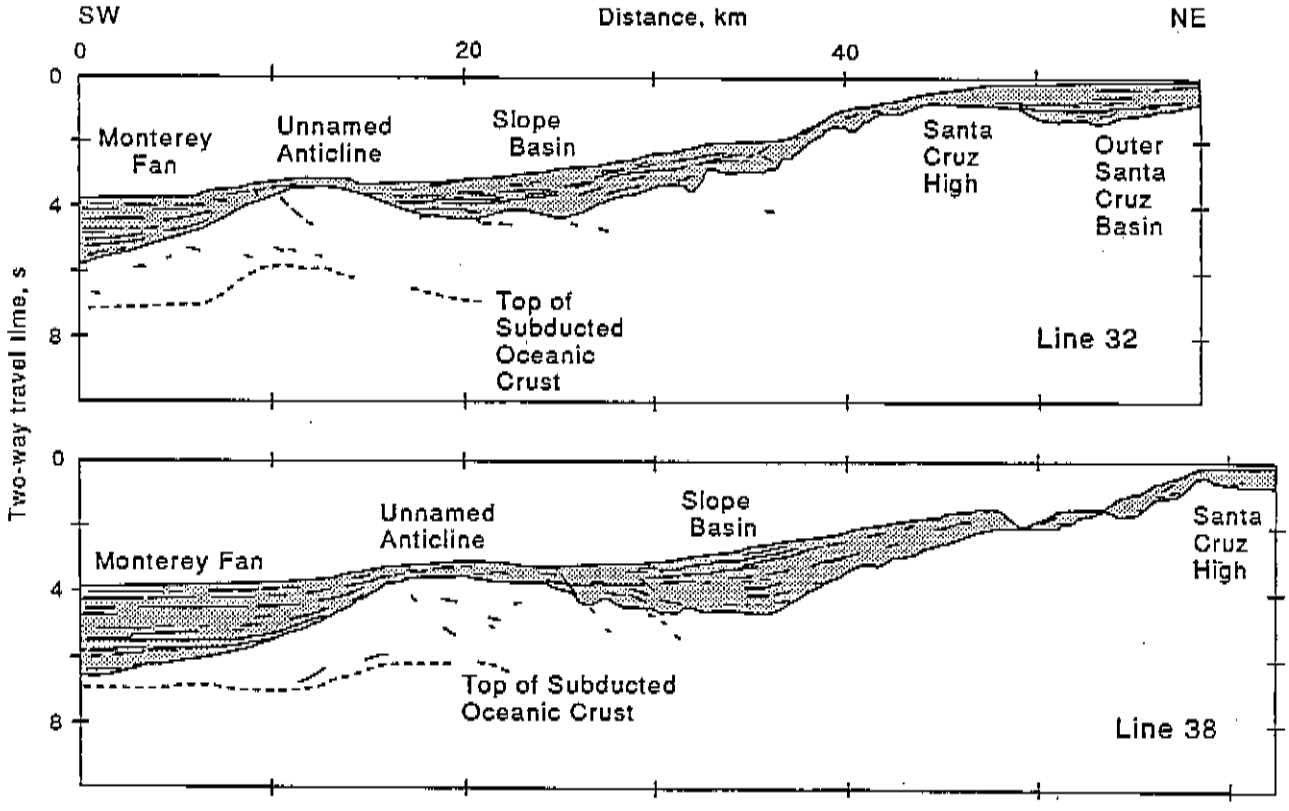

FIGURE 2. Line drawing interpretations of seismic reflection lines 32 and 38 showing the major structural elements revealed by these profiles. The seismic data were migrated; sections are plotted with a vertical exaggeration of about 1.78 for the Neogene sediments, shown as shaded.

DESCRIPTION OF THE DATA

Seismic reflection lines 32 and 38 image similar structural elements on the continental slope (fig. 2). Seaward of the Outer Santa Cruz basin and Santa Cruz high on the continental shelf, the lines image a thick slope basin locally containing more than 2000 m of sediments. These slope deposits thin over and are deformed by growth of an unnamed anticline at the base of the continental slope. Sediments of the Monterey deep-sea fan thin against, onlap, and appear to be uplifted by this unnamed anticline. Moderately dipping reflections from within the core of the anticline probably represent splay thrusts that dip landward. We interpret low-frequency reflections beneath the Neogene sediments as representing the top of the subducted oceanic crust of the Pacific plate.

Thirty-seven wide-angle seismic profiles (common receiver gathers), were recorded onshore during the acquisition of marine lines 32 and 38. Table 2 provides a list of stations that recorded each of these two lines as well as the source-receiver ranges provided by each receiver. Figures 3 to 39 provide examples of the records obtained by the receivers for both line 32 and 38, reduced using a velocity of 6 km/s and corrected for geometrical spreading by multiplying trace amplitudes by a factor of $\text{Range}^{0.7}$. Only records from the vertical seismometer component are presented in this report. In general, the signal-to-noise levels of the profiles are comparable to those obtained from similar experiments near Morro Bay, California (Trehu, 1991) and off central Oregon (Trehu and others, 1990), but are lower than those from the northern Gulf of Alaska (Brocher and Moses, 1990), where airgun array volumes between 3 to 5 times larger were used. Arrivals are sometimes difficult to identify; a few of the recorded profiles provide little useful information. As a rule, data quality improves as the distance of the station from the coast decreased; Station AN-1, on Waddell Creek near Ano Nuevo (fig. 1B), provided the highest-quality records of all stations (figs. 28 and 34). In general, the highest-quality wide-angle profiles were obtained in remote sites on or near bedrock exposures.

TABLE 2. Wide-angle Seismic Profiles

Line 32

Site No.	Recorded Ranges (km)
LP-1	21.6-74.6
LP-2	25.0-80.1
LP-3	33.7-88.3
LP-4	38.8-94.9
LP-5	46.7-103.6
LP-6	52.7-110.6
LP-7	56.0-114.9
LP-8	65.5-124.9
LP-9	69.8-129.5
LP-10	80.5-140.5
LP-11	89.3-149.3
LP-12	96.3-156.9
AN-1	10.5-71.9
AN-2	18.3-79.6
AN-3	30.4-91.8
AN-4	66.7-128.2
AN-5	76.6-138.1
AN-6	89.4-150.8

TABLE 2. Continued.

Line 38

Site No.	Recorded Ranges (km)
LP-1	11.0-72.7
LP-2	16.7-78.4
LP-3	24.2-85.6
LP-4	31.0-92.4
LP-5	39.6-101.0
LP-6	46.7-108.2
LP-7	51.5-113.1
LP-8	61.7-123.3
LP-9	66.3-128.0
LP-10	77.4-139.1
LP-11	86.1-147.8
LP-12	94.3-156.0
LP-13	103.3-165.0
AN-1	21.0-74.6
AN-2	25.3-82.0
AN-3	35.4-94.0
AN-4	69.8-130.2
AN-5	79.6-140.1
AN-6	91.0-152.1

The wide-angle records obtained along the Loma Prieta and Ano Nuevo transects show six characteristic arrivals (figs. 3-39). The first of these are secondary arrivals having a velocity between 1.7 and 2.0 km/s that are observed at stations near the coast to source-receiver offsets as large as 30 km. The second group of arrivals are refractions from the upper crust (Pg) which are observed to source-receiver ranges in excess of 100 km (figs. 12 and 32). At the nearest ranges the Pg arrivals have apparent velocities of 4 to 5 km/s and at greater ranges these abruptly increase to 6 km/s. At the farther ranges the travel times of the Pg arrivals clearly show the influence of the topography of the outer margin and continental slope (fig. 2), which cause undulations in Pg travel times up to 0.4 seconds. A third group of arrivals is represented by weaker wide-angle reflections from the mid-crust are observed on the highest quality profiles (e.g., fig. 4). A fourth set of arrivals is represented by reflections from the top of the upper mantle, the Moho, and is designated as PmP. These arrivals are interpreted as PmP because they are normally the strongest secondary arrivals observed on the records, and because they frequently display the largest amplitudes of all recorded arrivals. Refractions from the upper mantle, Pn arrivals, are generally observed but due to complex structure do not generally show velocities typical of the upper mantle. The sixth and last type of arrival is represented by secondary arrivals having a linear moveout and an apparent velocity of 2.7 km/s. These arrivals probably represent shear waves converted near the base of the thin sedimentary blanket covering the upper continental slope. A preliminary interpretation of these data was presented by Brocher and others (1991).

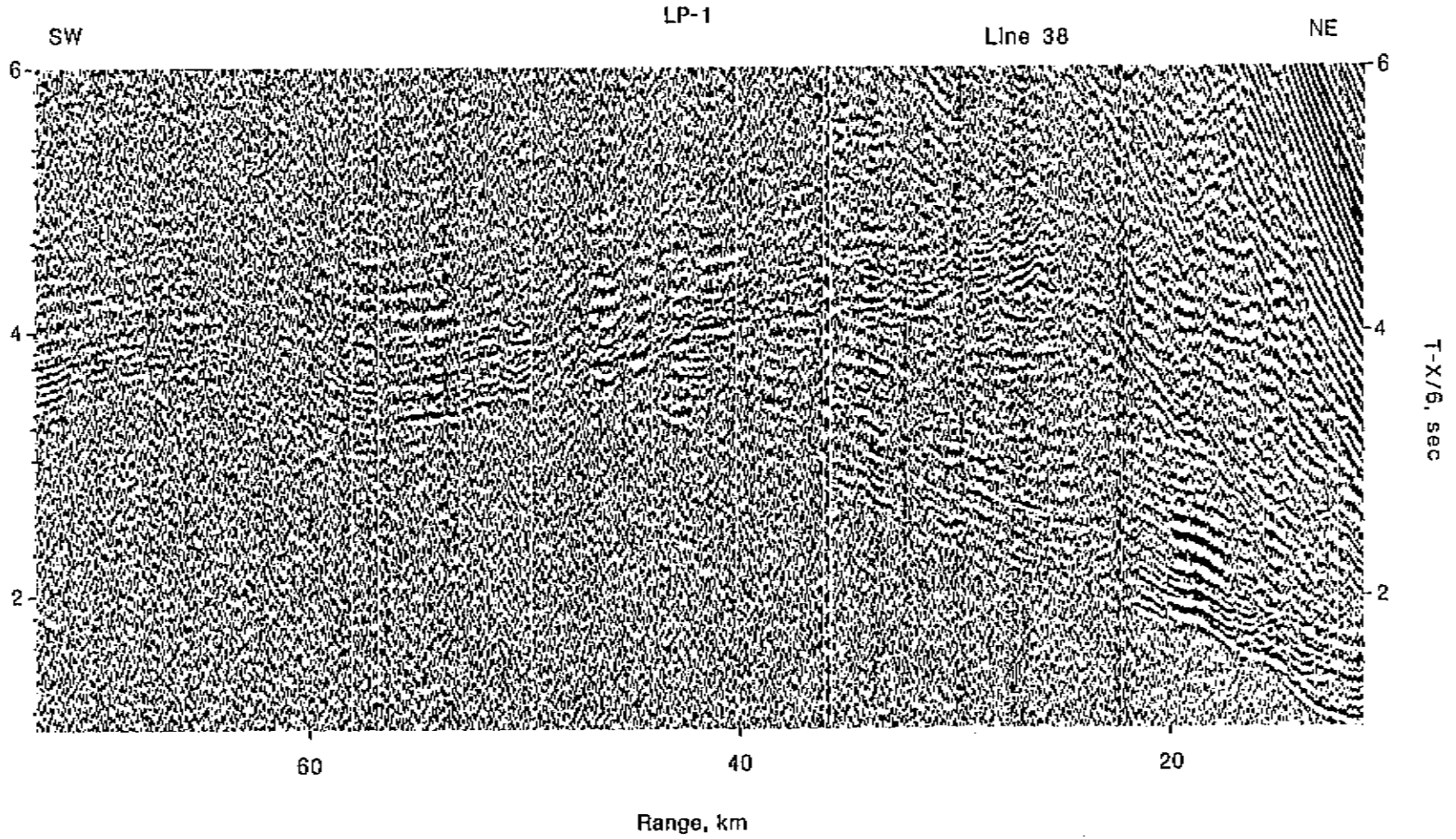

FIGURE 3. Receiver gather LP-1 from line 38. The record section has been linearly reduced using a velocity of 6 km/s and trace amplitudes have been scaled according to Range$^{0.7}$. A few noisy traces have been deleted.

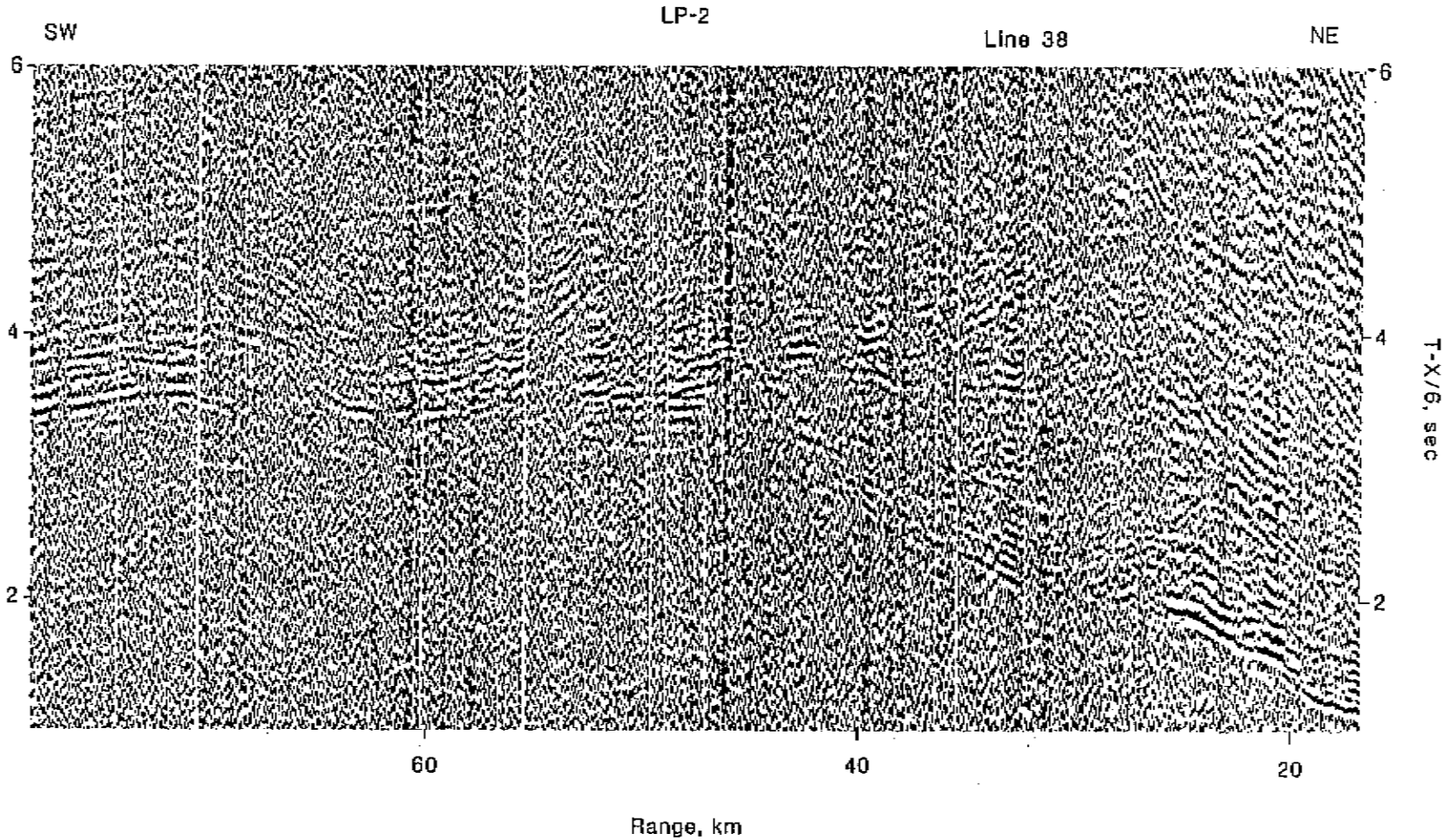

FIGURE 4. Receiver gather LP-2 from line 38. The record section has been linearly reduced using a velocity of 6 km/s and trace amplitudes have been scaled according to Range$^{0.7}$. A few noisy traces have been deleted.

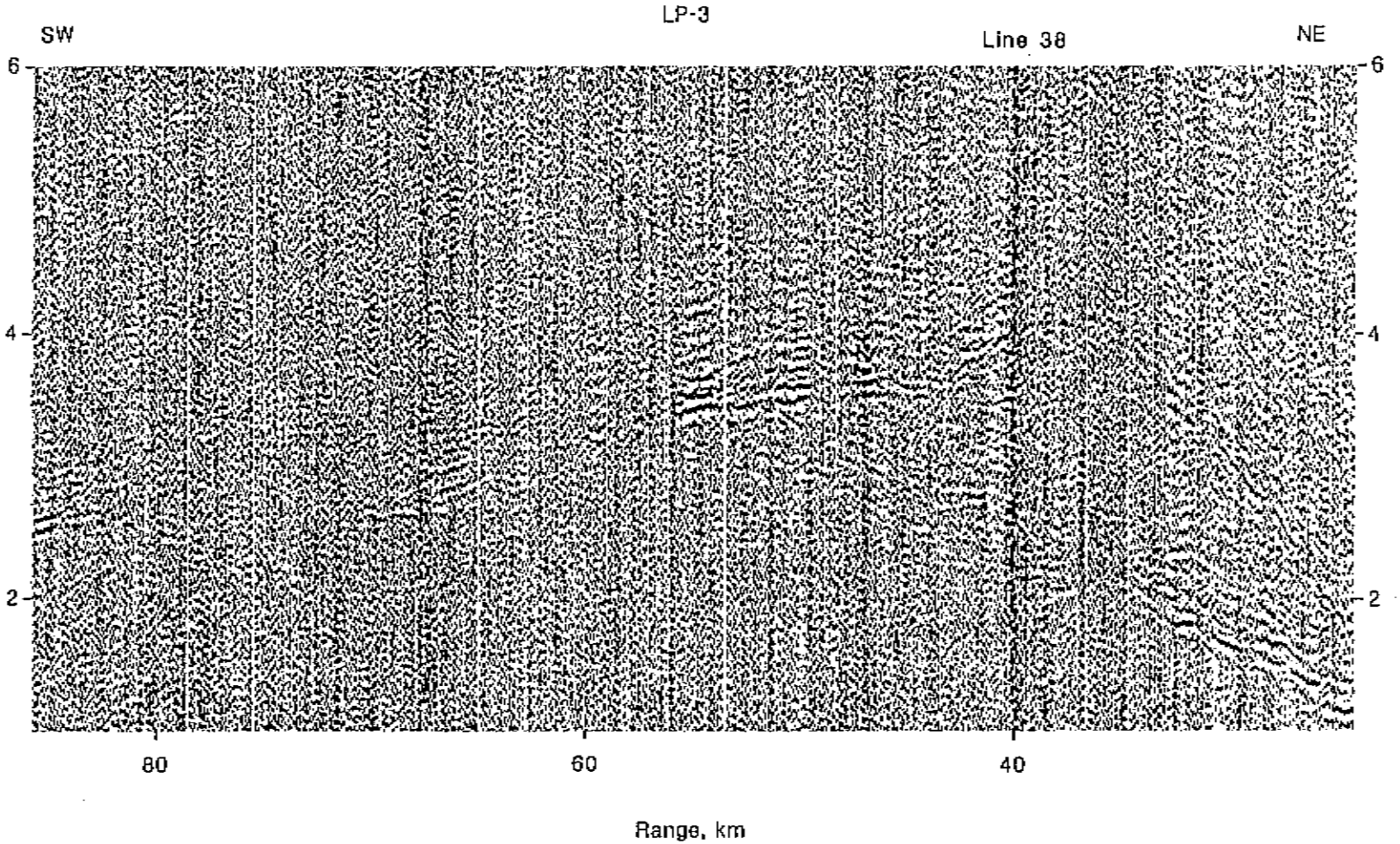

FIGURE 5. Receiver gather LP-3 from line 38. The record section has been linearly reduced using a velocity of 6 km/s and trace amplitudes have been scaled according to Range$^{0.7}$. A few noisy traces have been deleted.

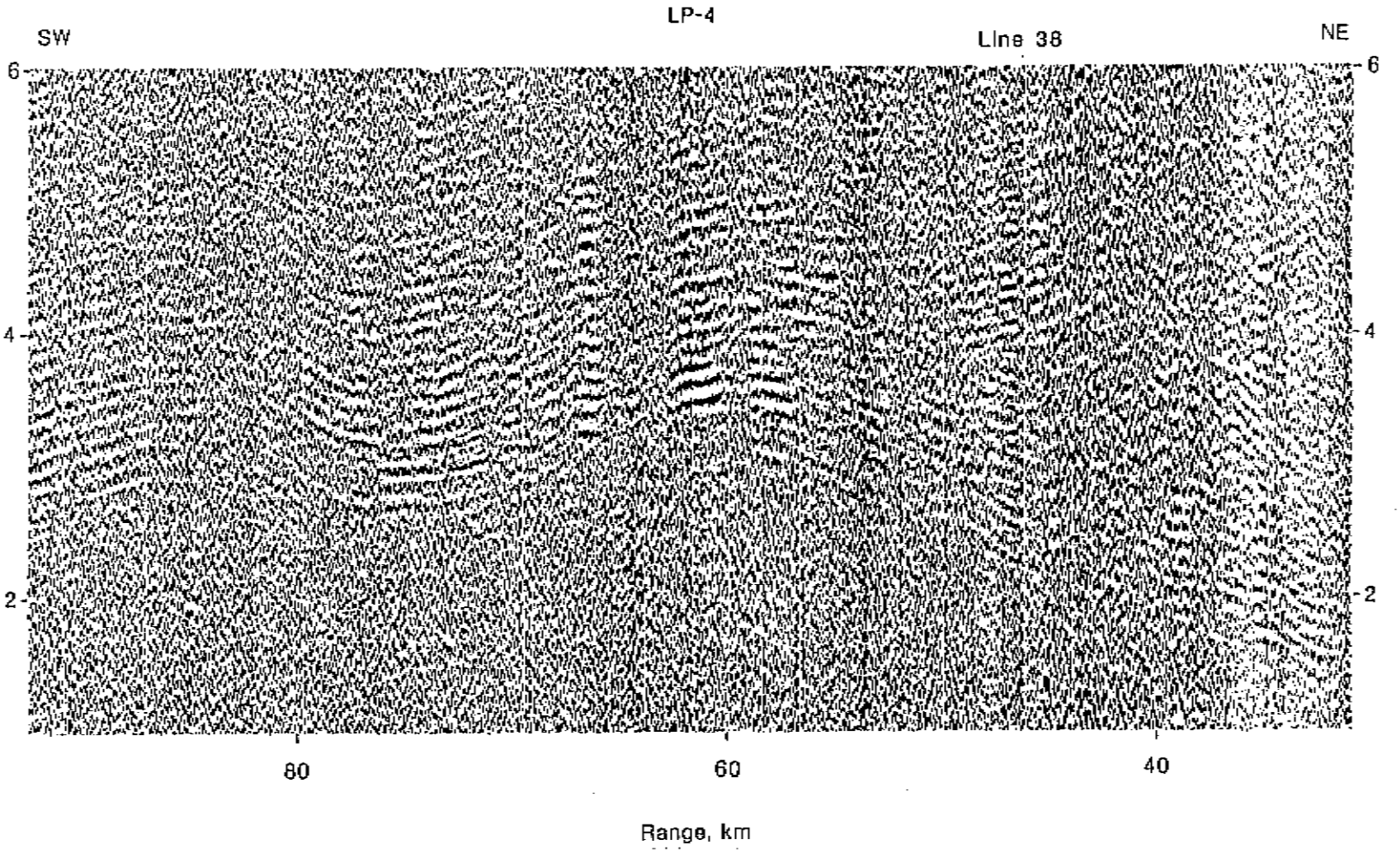

FIGURE 6. Receiver gather LP-4 from line 38. The record section has been linearly reduced using a velocity of 6 km/s and trace amplitudes have been scaled according to Range$^{0.7}$. A few noisy traces have been deleted.

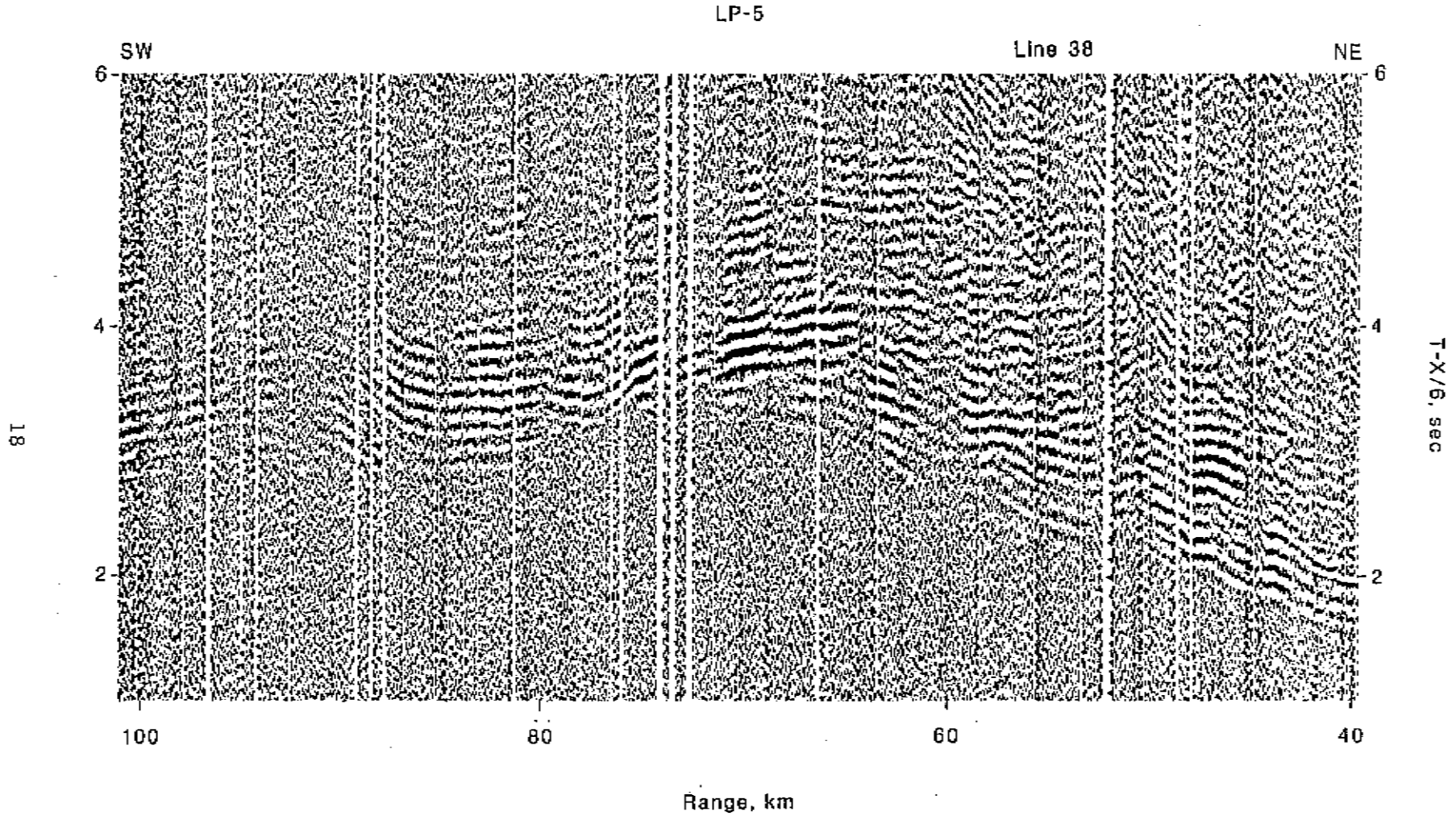

FIGURE 7. Receiver gather LP-5 from line 38. The record section has been linearly reduced using a velocity of 6 km/s and trace amplitudes have been scaled according to Range$^{0.7}$. A few noisy traces have been deleted.

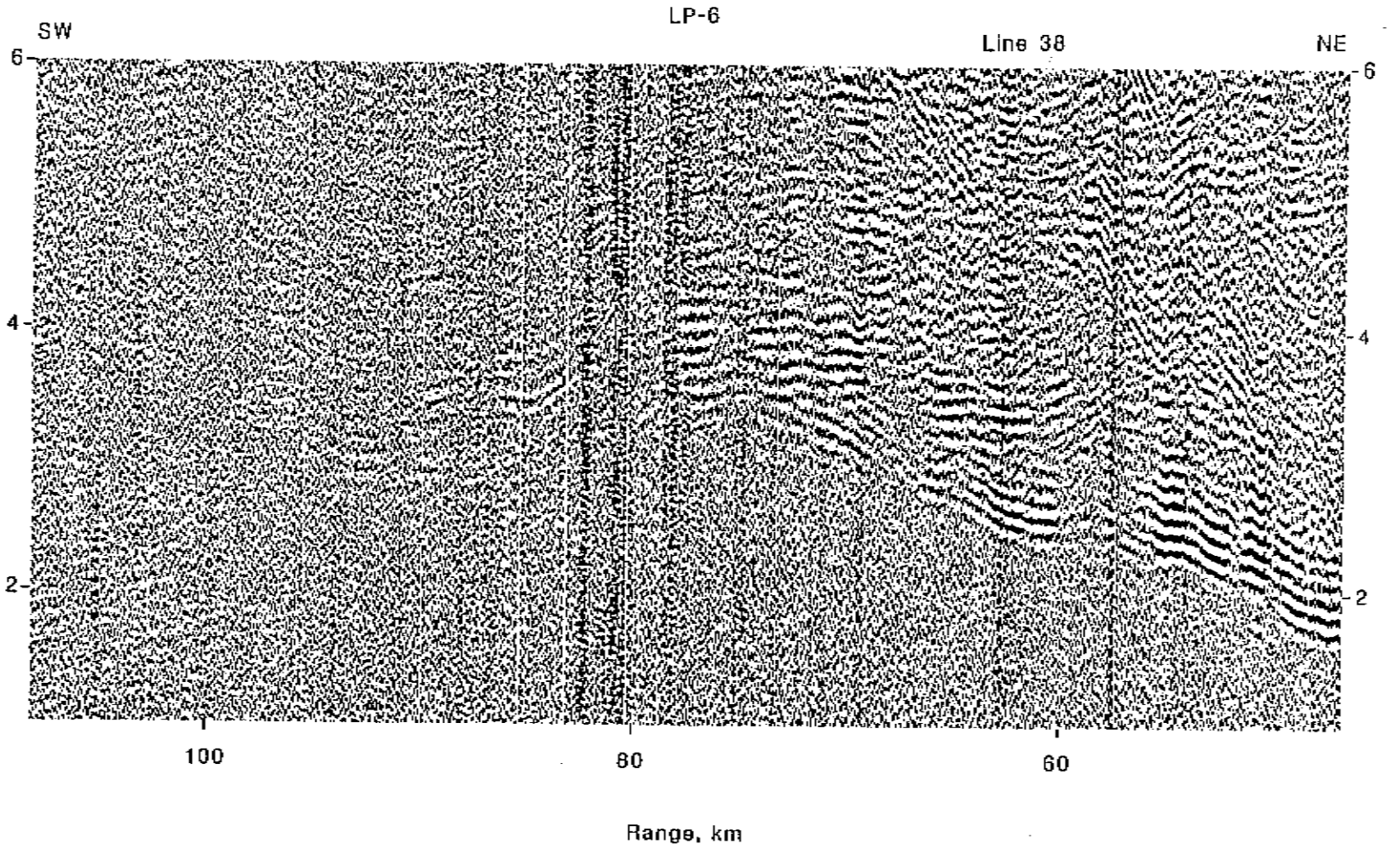

FIGURE 8. Receiver gather LP-6 from line 38. The record section has been linearly reduced using a velocity of 6 km/s and trace amplitudes have been scaled according to Range$^{0.7}$. A few noisy traces have been deleted.

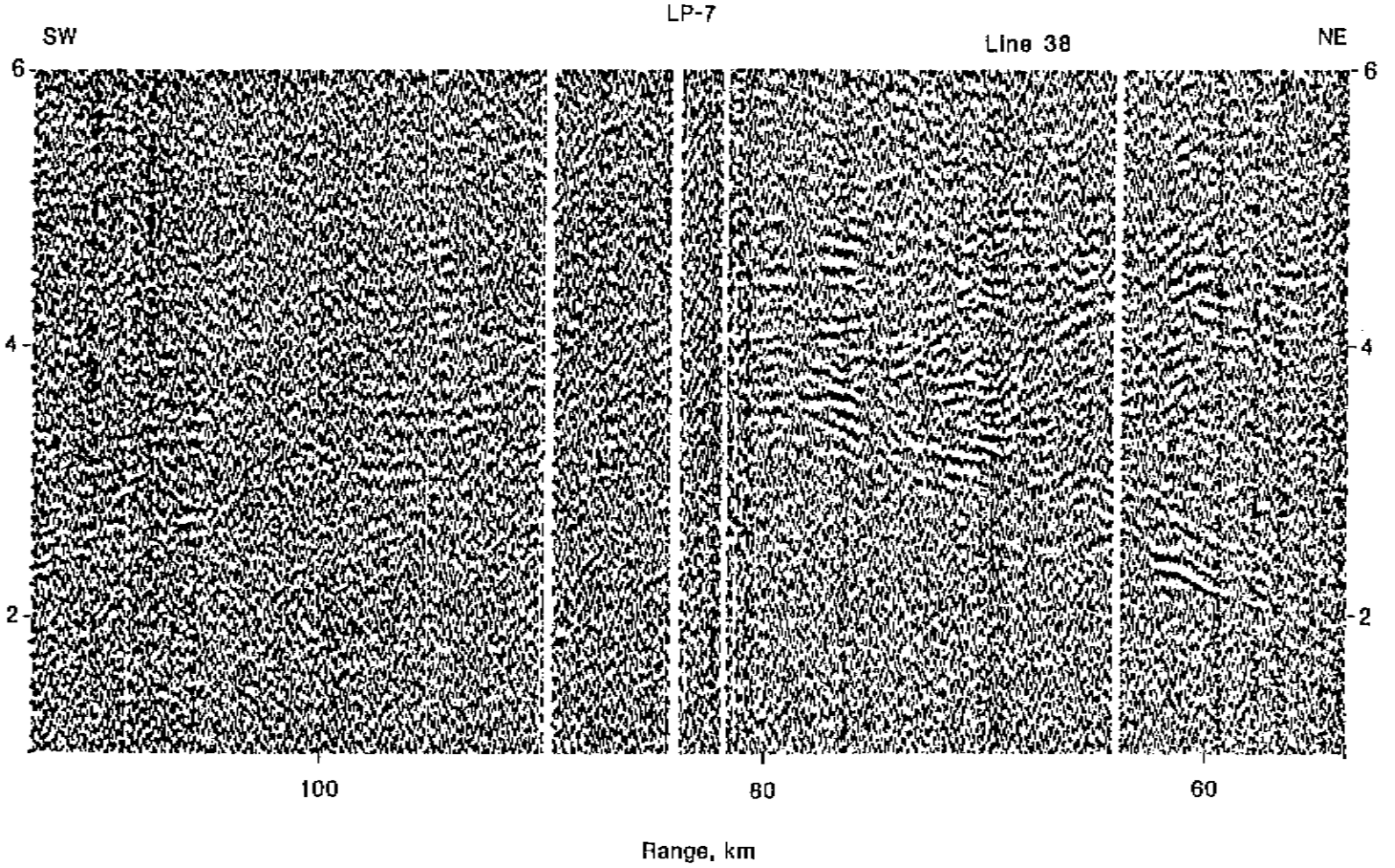

FIGURE 9. Receiver gather LP-7 from line 38. The record section has been linearly reduced using a velocity of 6 km/s and trace amplitudes have been scaled according to Range$^{0.7}$. A few noisy traces have been deleted.

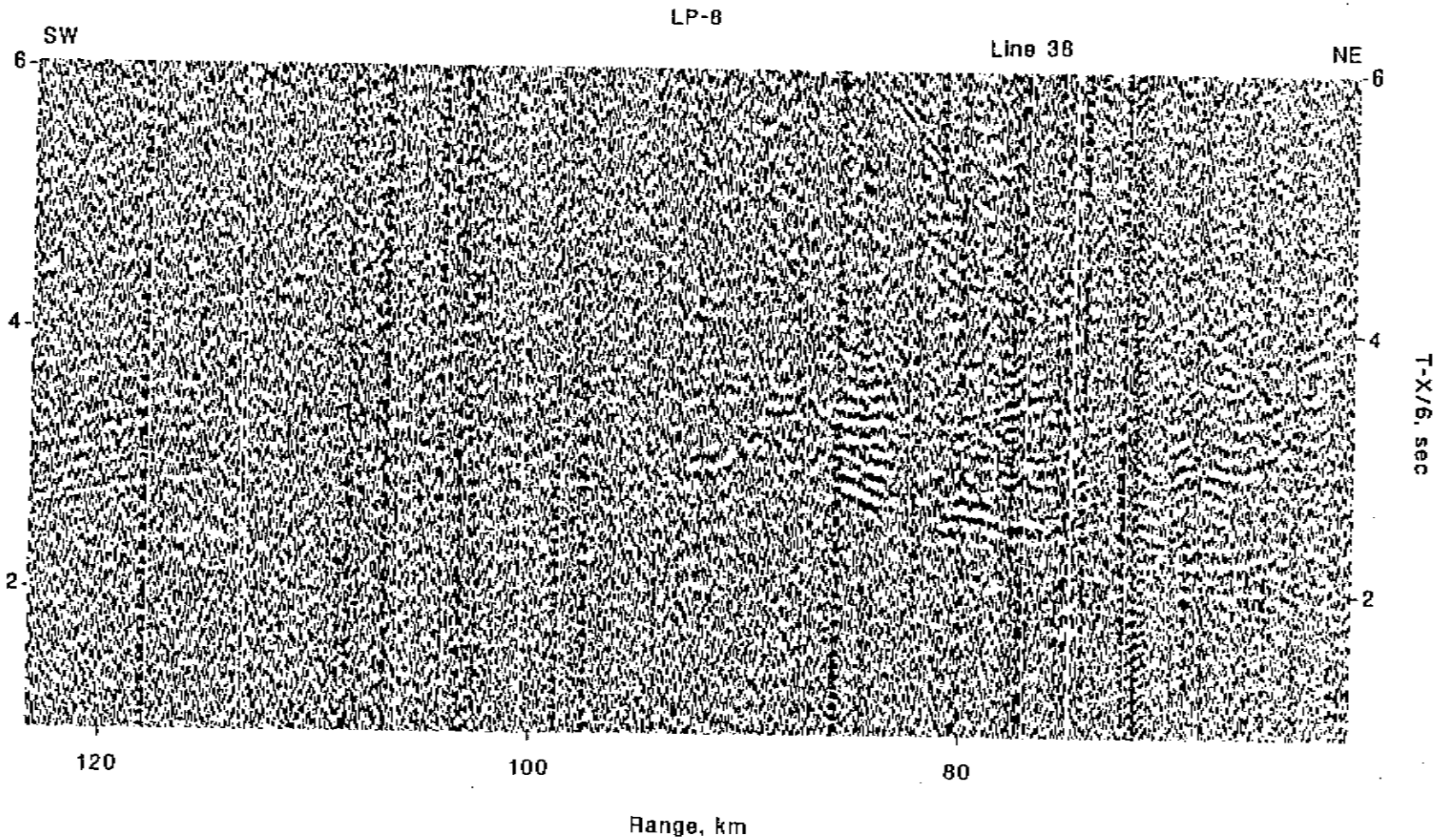

FIGURE 10. Receiver gather LP-8 from line 38. The record section has been linearly reduced using a velocity of 6 km/s and trace amplitudes have been scaled according to Range$^{0.7}$. A few noisy traces have been deleted.

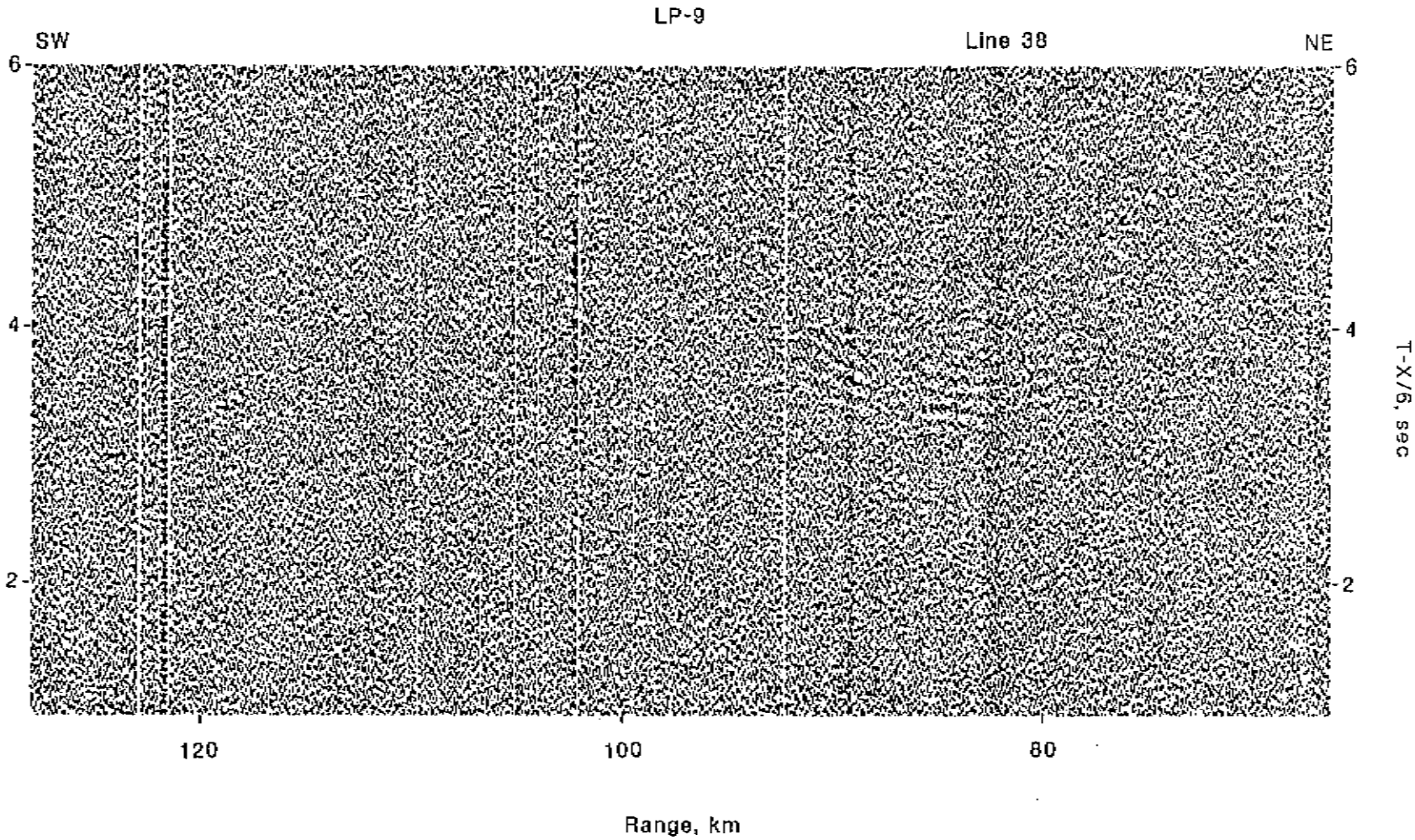

FIGURE 11. Receiver gather LP-9 from line 38. The record section has been linearly reduced using a velocity of 6 km/s and trace amplitudes have been scaled according to Range$^{0.7}$. A few noisy traces have been deleted.

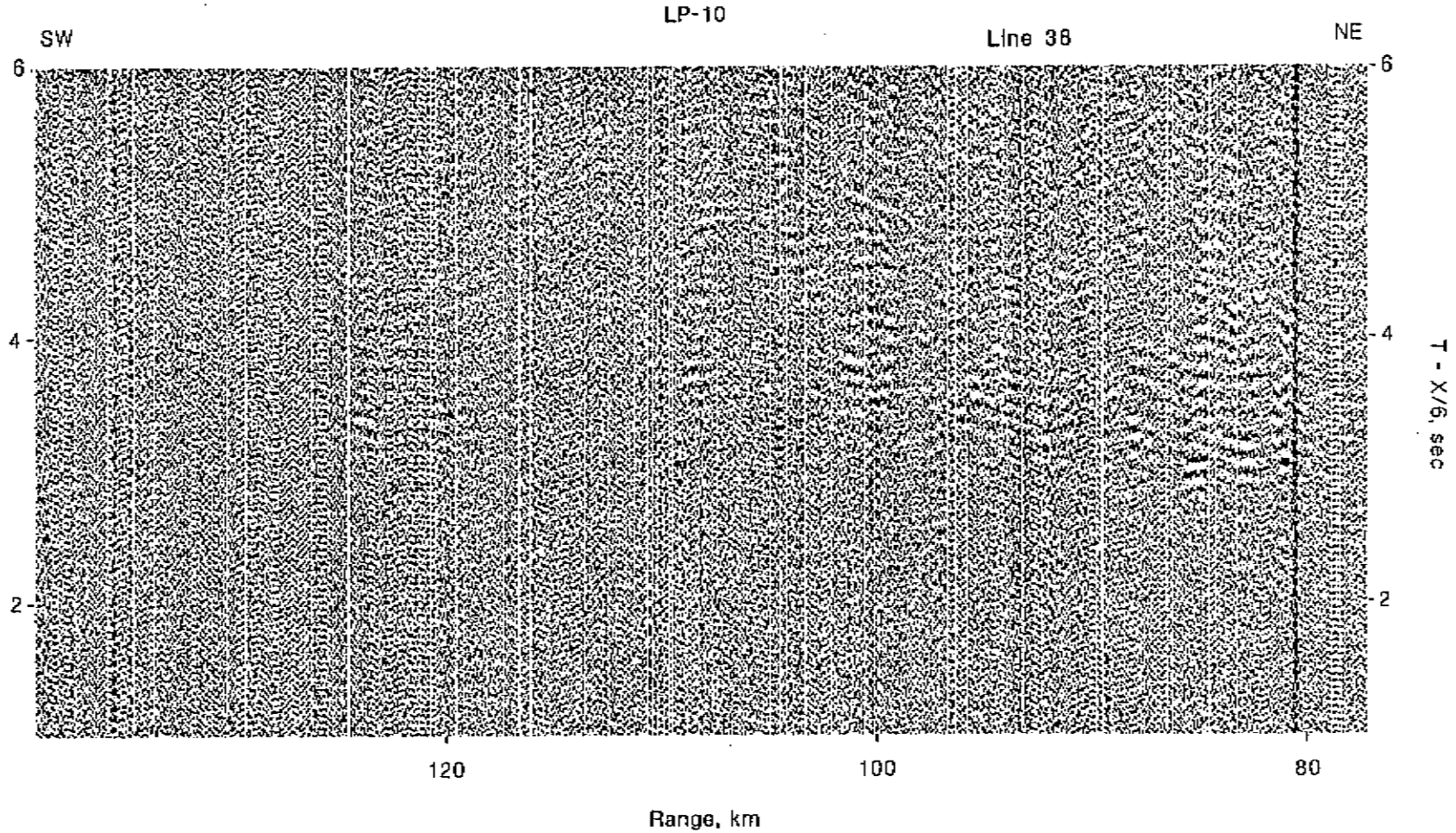

FIGURE 12. Receiver gather recorded at Station LP-10 for line 38. The record section has been linearly reduced using a velocity of 6 km/s and trace amplitudes have been scaled according to Range$^{0.7}$. A few noisy traces have been deleted.

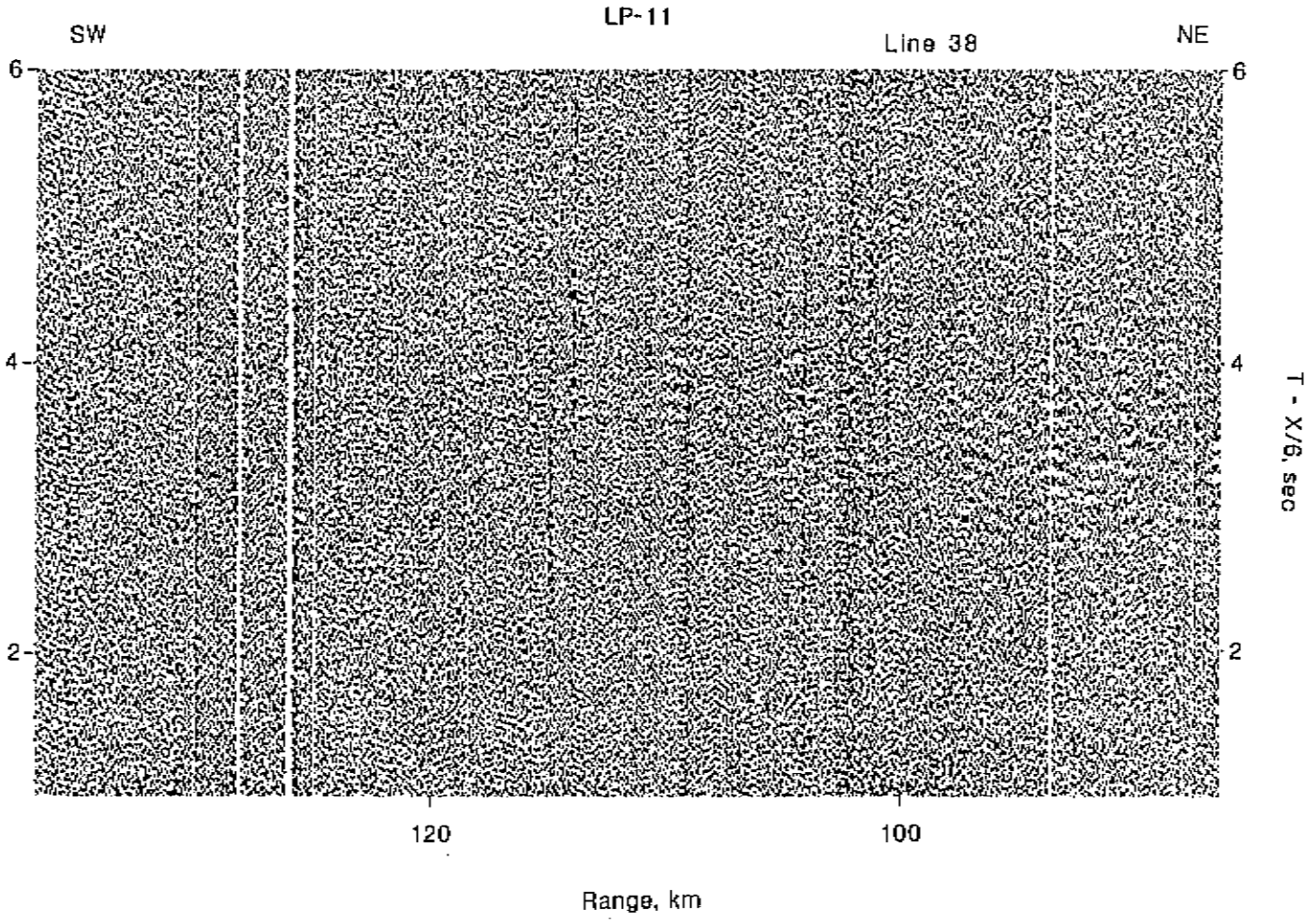

FIGURE 13. Receiver gather LP-11 from line 38. The record section has been linearly reduced using a velocity of 6 km/s and trace amplitudes have been scaled according to Range$^{0.7}$. A few noisy traces have been deleted.

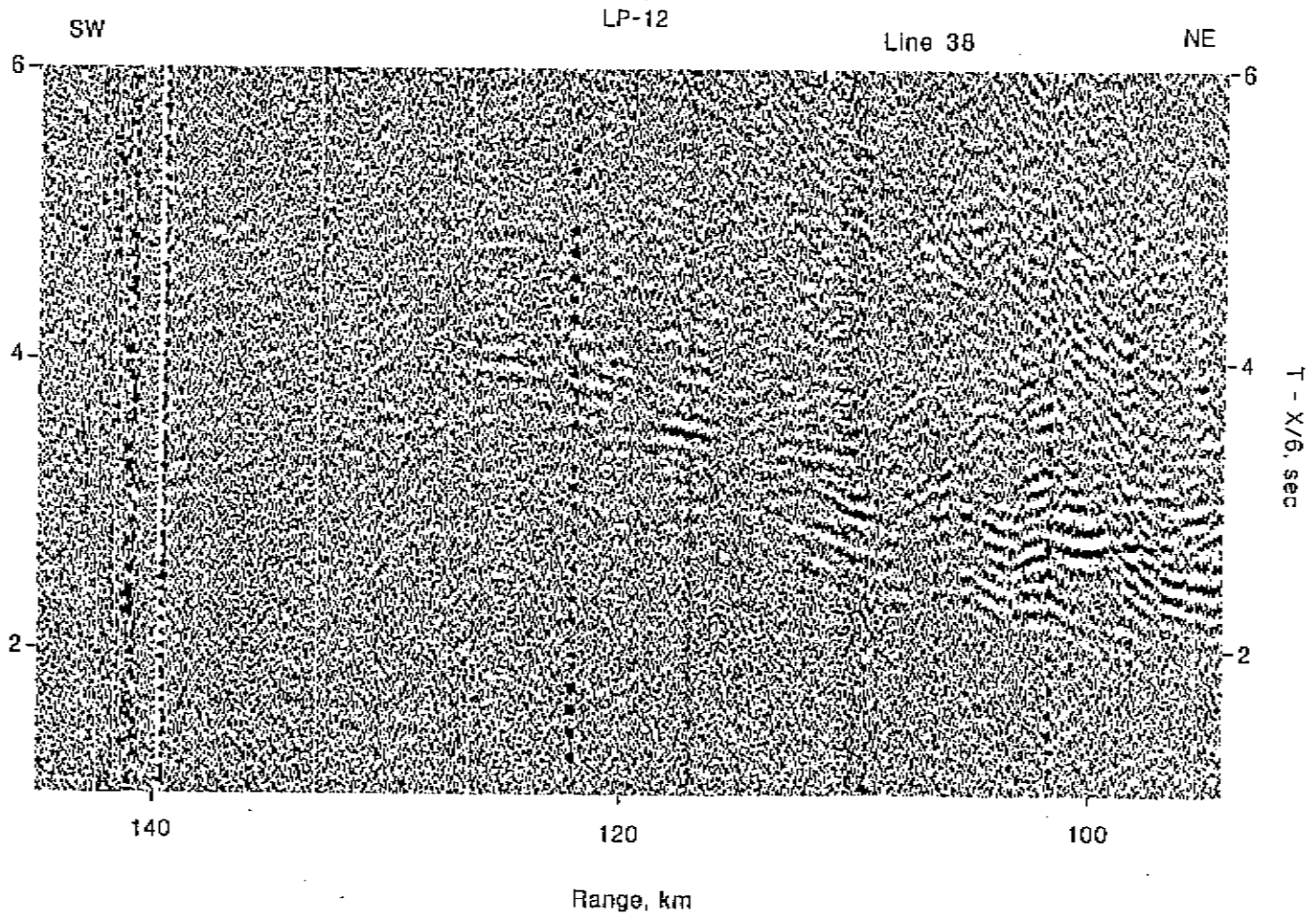

FIGURE 14. Receiver gather LP-12 from line 38. The record section has been linearly reduced using a velocity of 6 km/s and trace amplitudes have been scaled according to Range$^{0.7}$. A few noisy traces have been deleted.

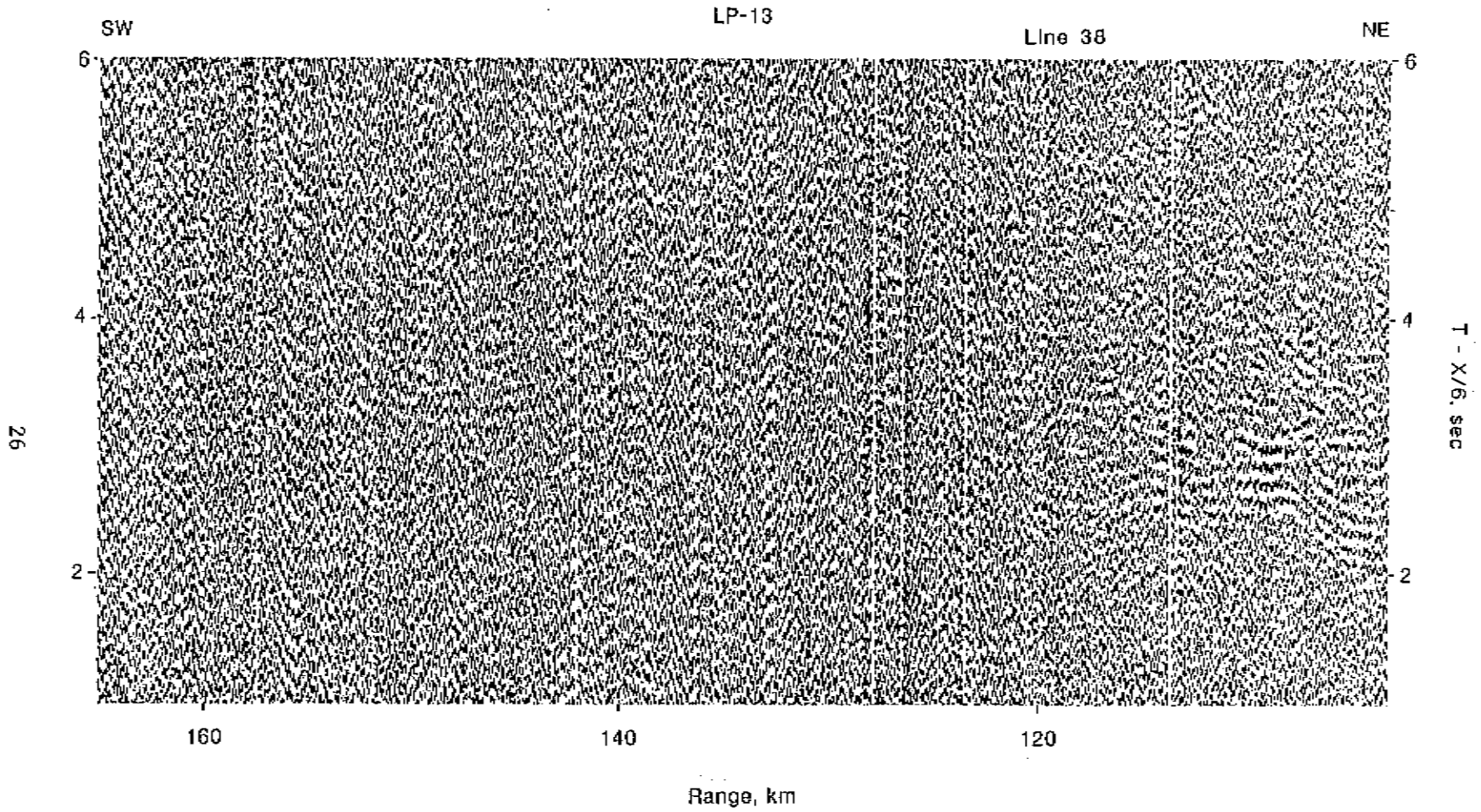

FIGURE 15. Receiver gather LP-13 from line 38. The record section has been linearly reduced using a velocity of 6 km/s and trace amplitudes have been scaled according to Range$^{0.7}$. A few noisy traces have been deleted.

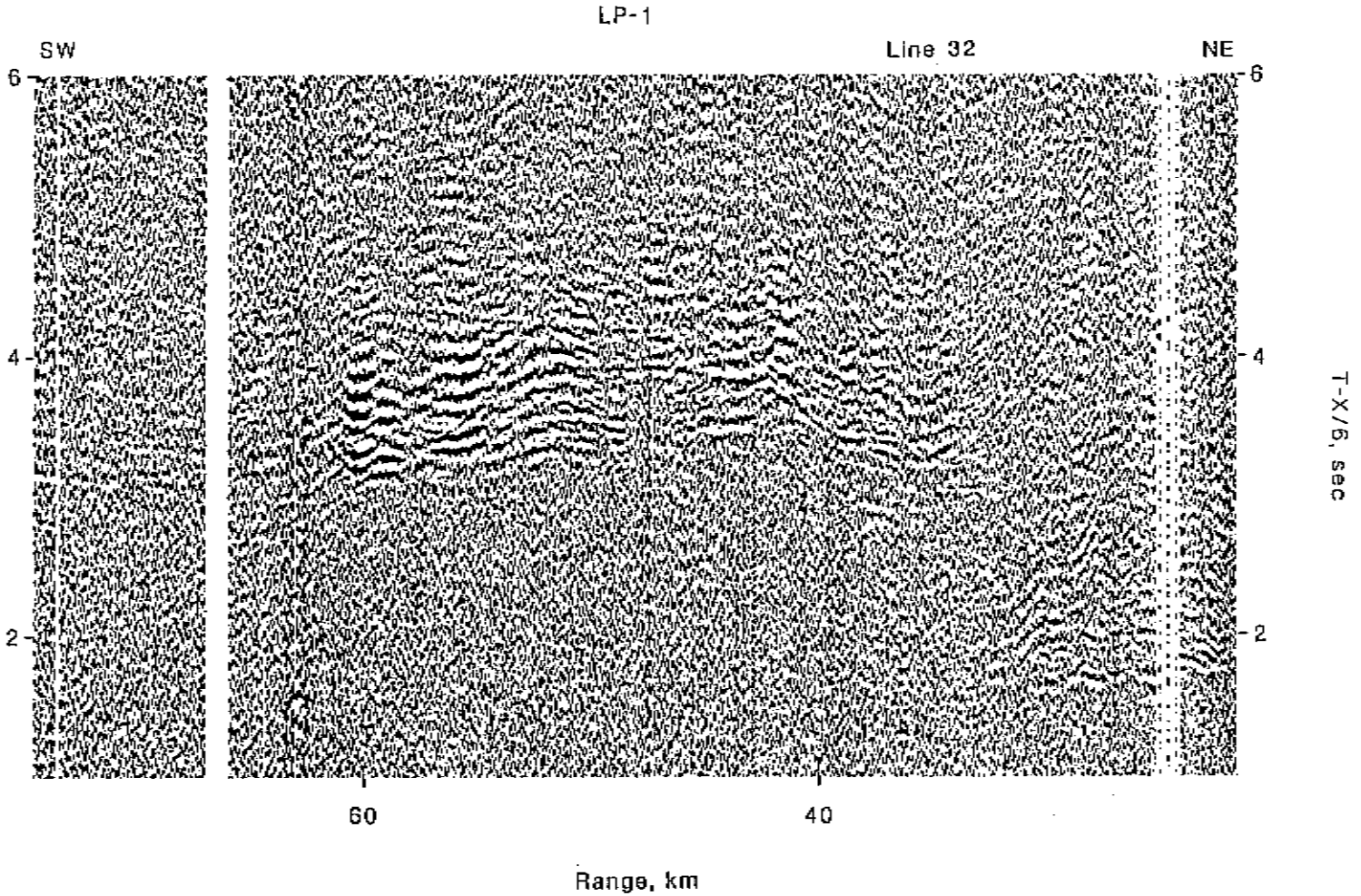

FIGURE 16. Receiver gather LP-1 from line 32. The record section has been linearly reduced using a velocity of 6 km/s and trace amplitudes have been scaled according to Range$^{0.7}$. A few noisy traces have been deleted.

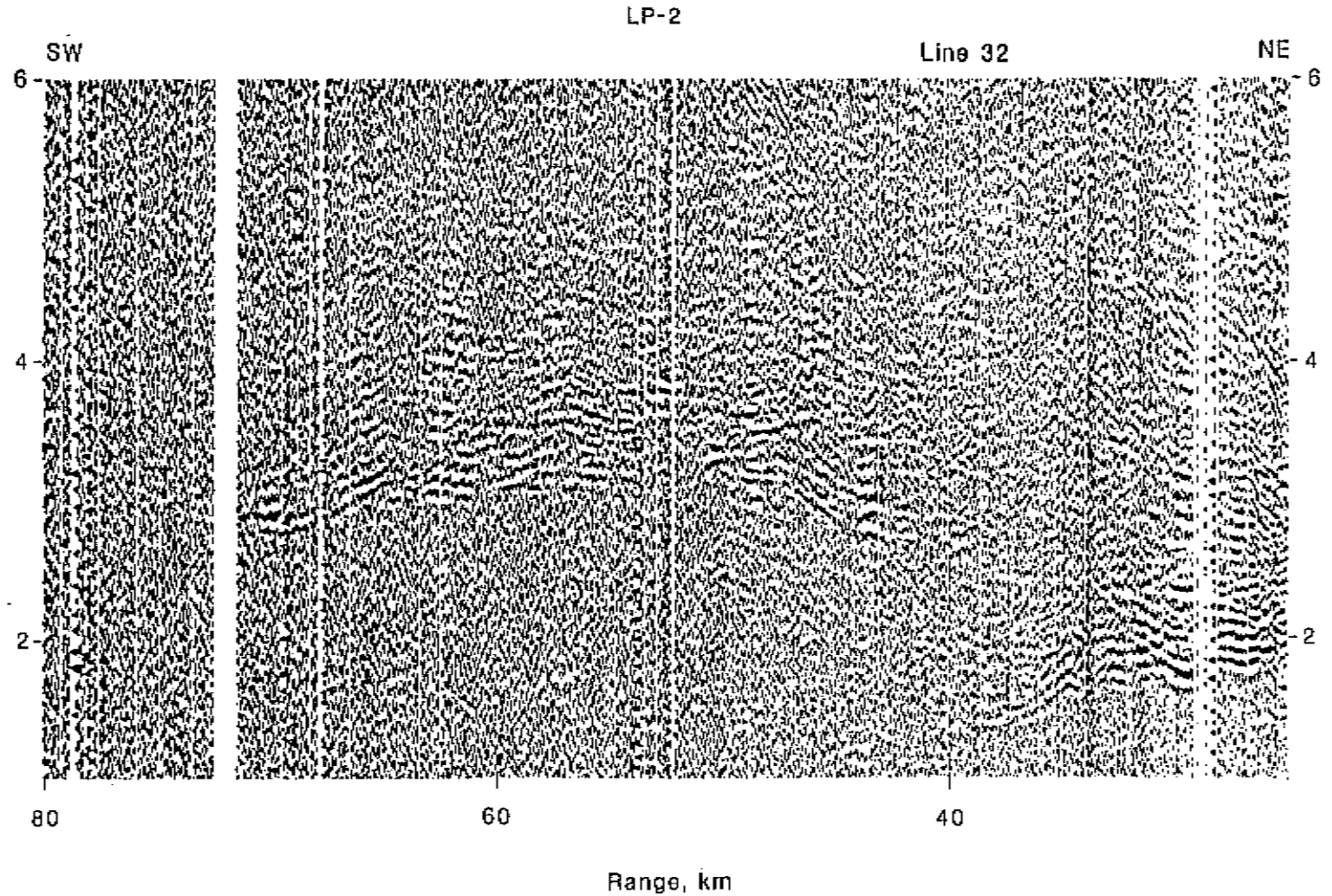

FIGURE 17. Receiver gather LP-2 from line 32. The record section has been linearly reduced using a velocity of 6 km/s and trace amplitudes have been scaled according to Range$^{0.7}$. A few noisy traces have been deleted.

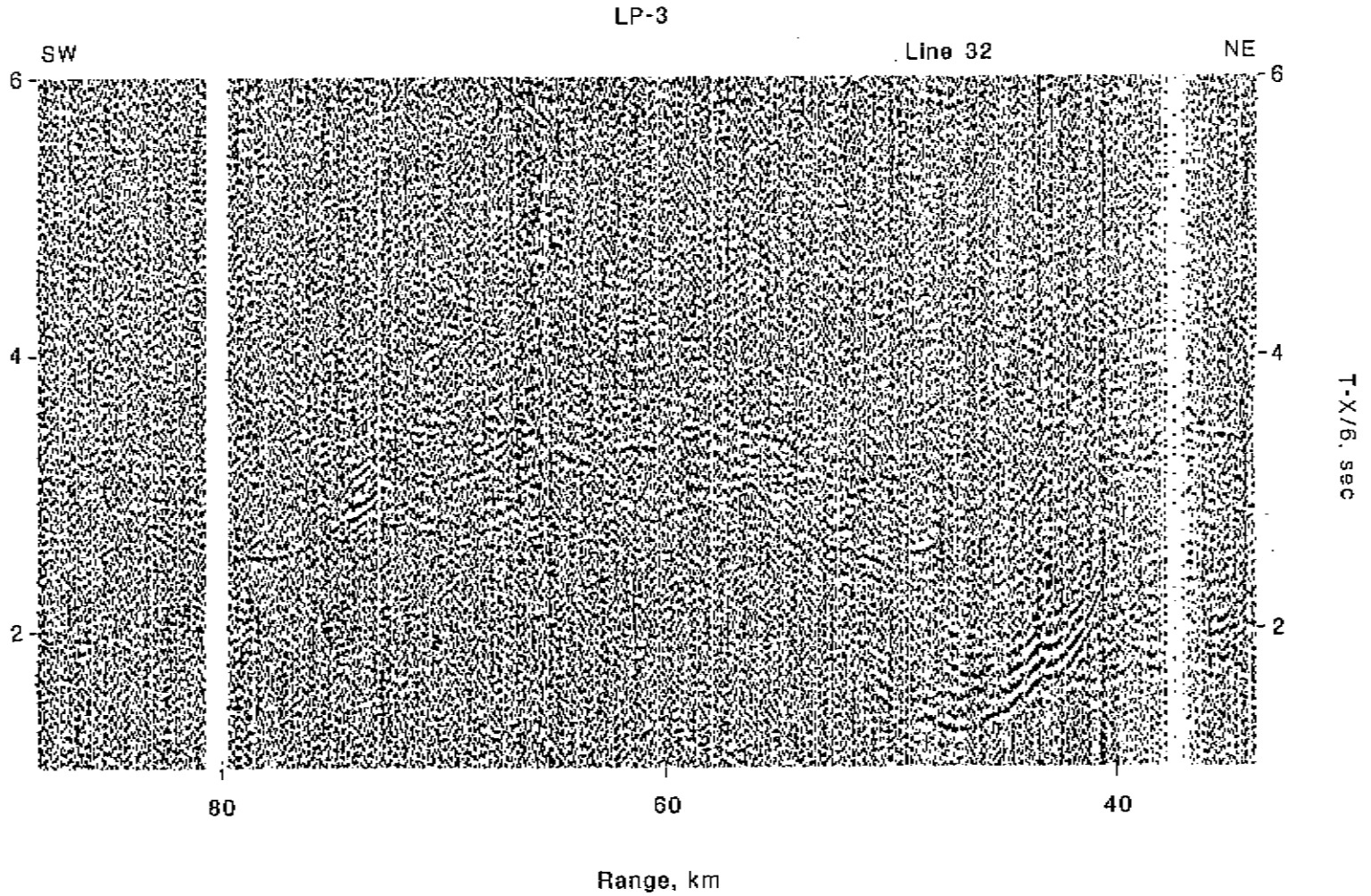

FIGURE 18. Receiver gather LP-3 from line 32. The record section has been linearly reduced using a velocity of 6 km/s and trace amplitudes have been scaled according to Range$^{0.7}$. A few noisy traces have been deleted.

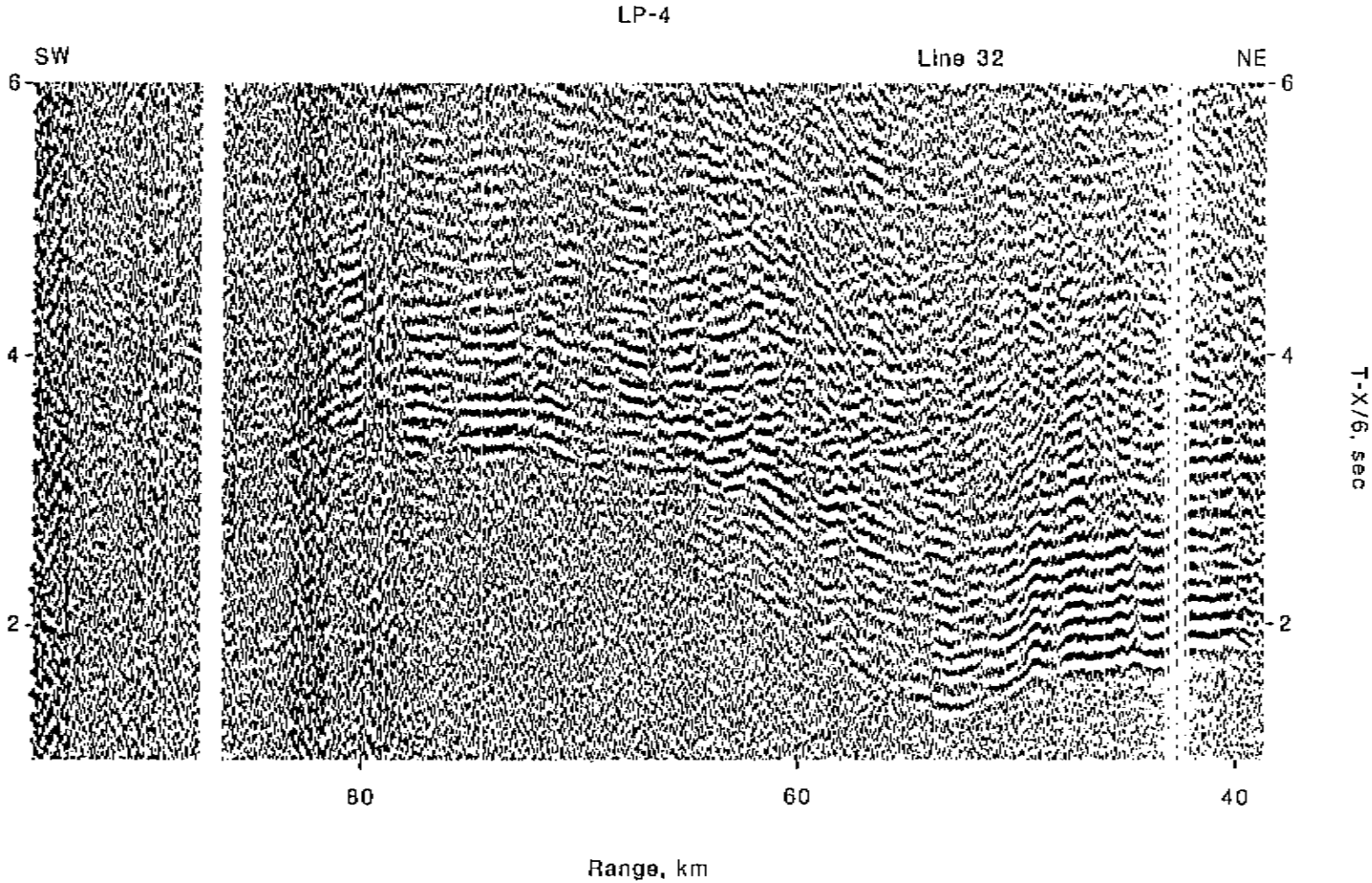

FIGURE 19. Receiver gather LP-4 from line 32. The record section has been linearly reduced using a velocity of 6 km/s and trace amplitudes have been scaled according to Range$^{0.7}$. A few noisy traces have been deleted.

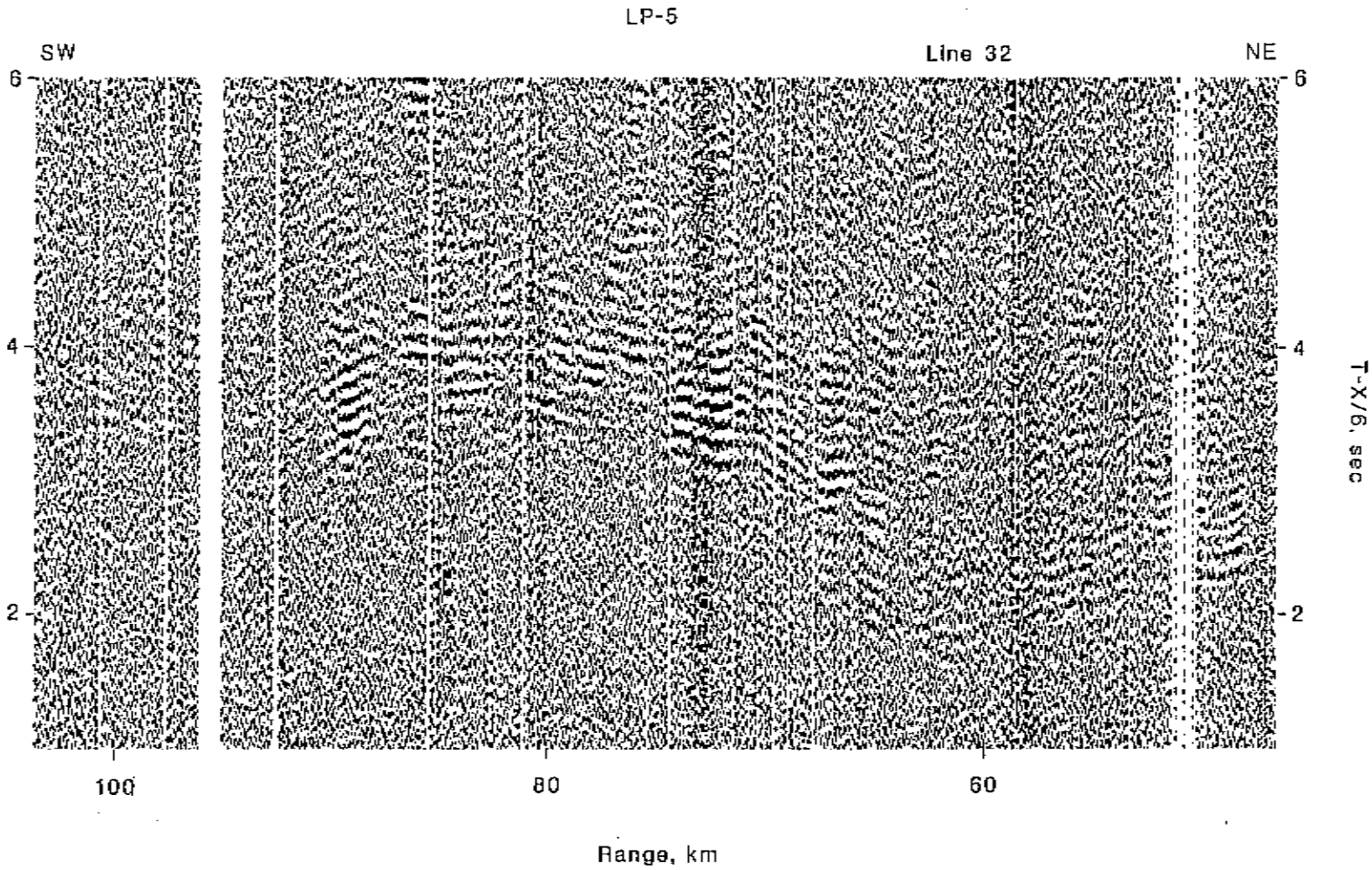

FIGURE 20. Receiver gather LP-5 from line 32. The record section has been linearly reduced using a velocity of 6 km/s and trace amplitudes have been scaled according to Range$^{0.7}$. A few noisy traces have been deleted.

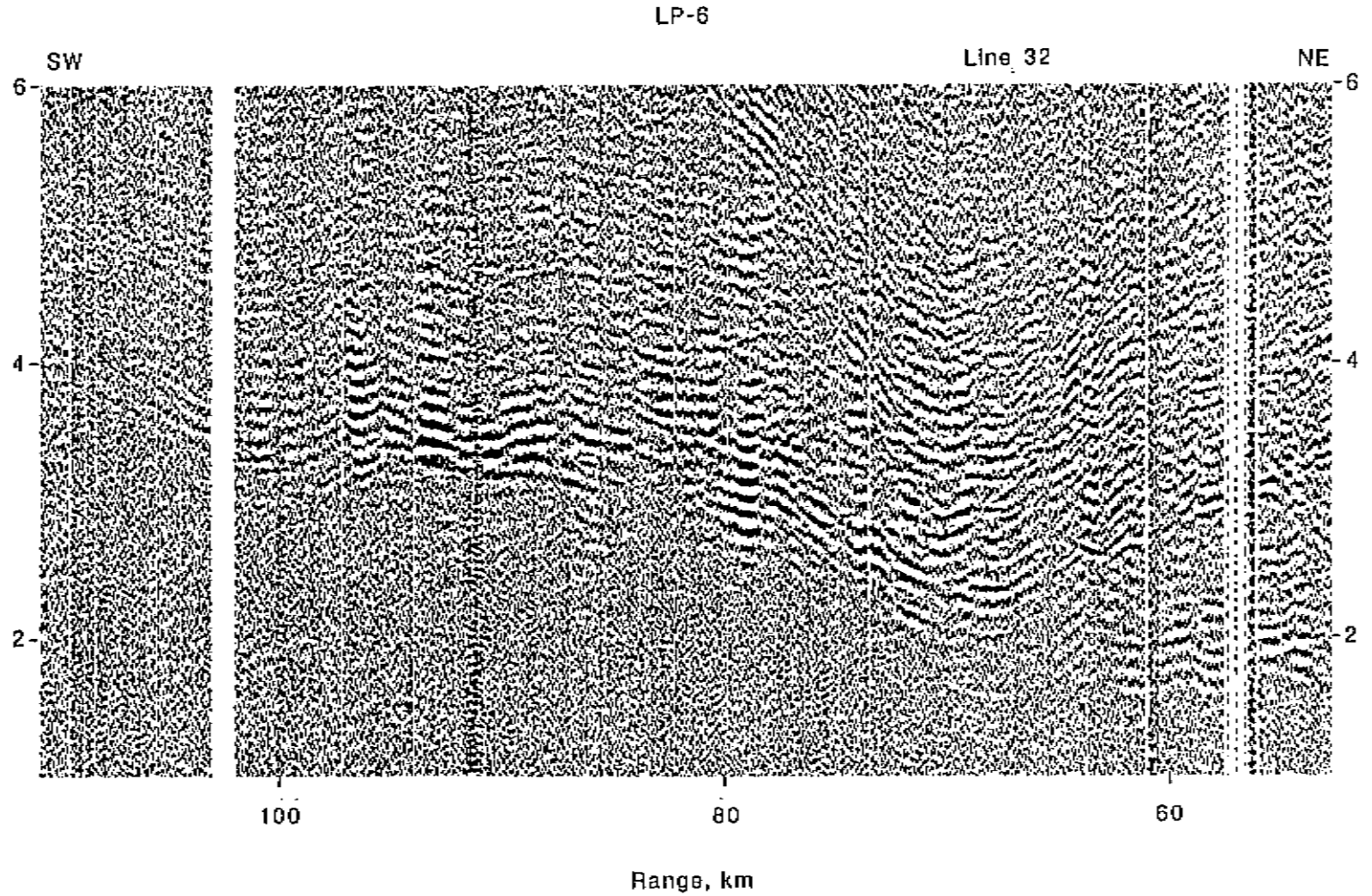

FIGURE 21. Receiver gather LP-6 from line 32. The record section has been linearly reduced using a velocity of 6 km/s and trace amplitudes have been scaled according to Range$^{0.7}$. A few noisy traces have been deleted.

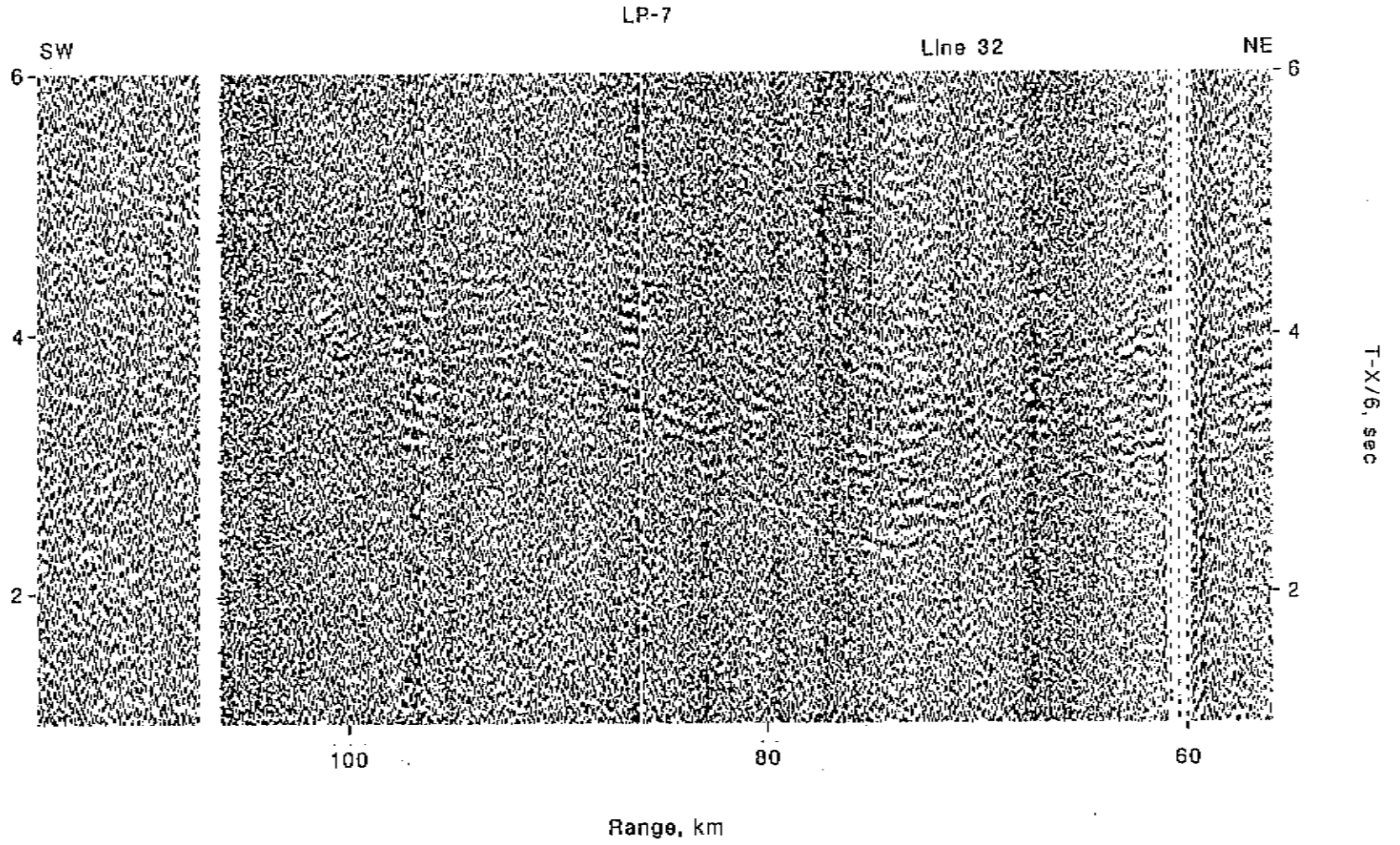

FIGURE 22. Receiver gather LP-7 from line 32. The record section has been linearly reduced using a velocity of 6 km/s and trace amplitudes have been scaled according to Range$^{0.7}$. A few noisy traces have been deleted.

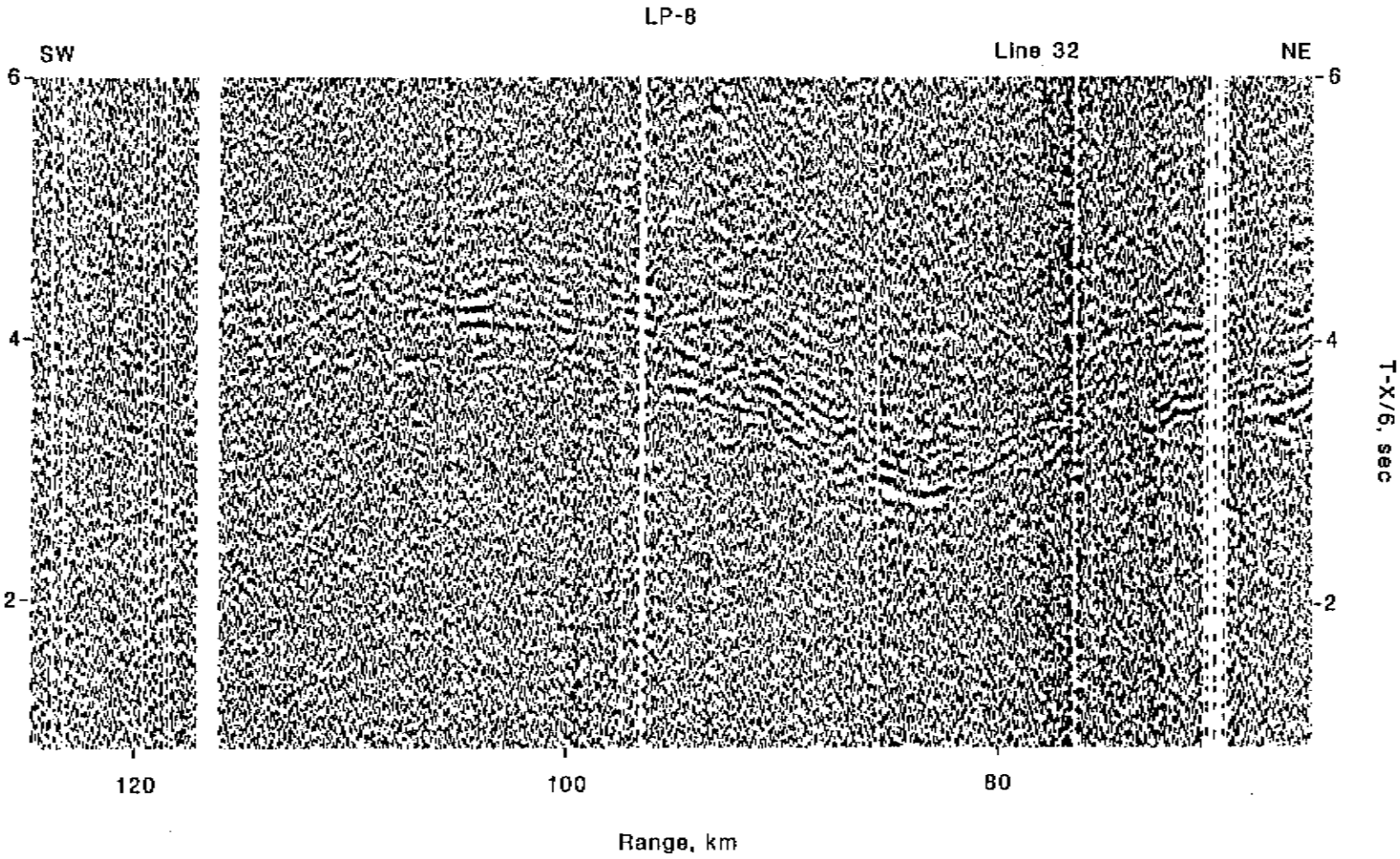

FIGURE 23. Receiver gather LP-8 from line 32. The record section has been linearly reduced using a velocity of 6 km/s and trace amplitudes have been scaled according to Range$^{0.7}$. A few noisy traces have been deleted.

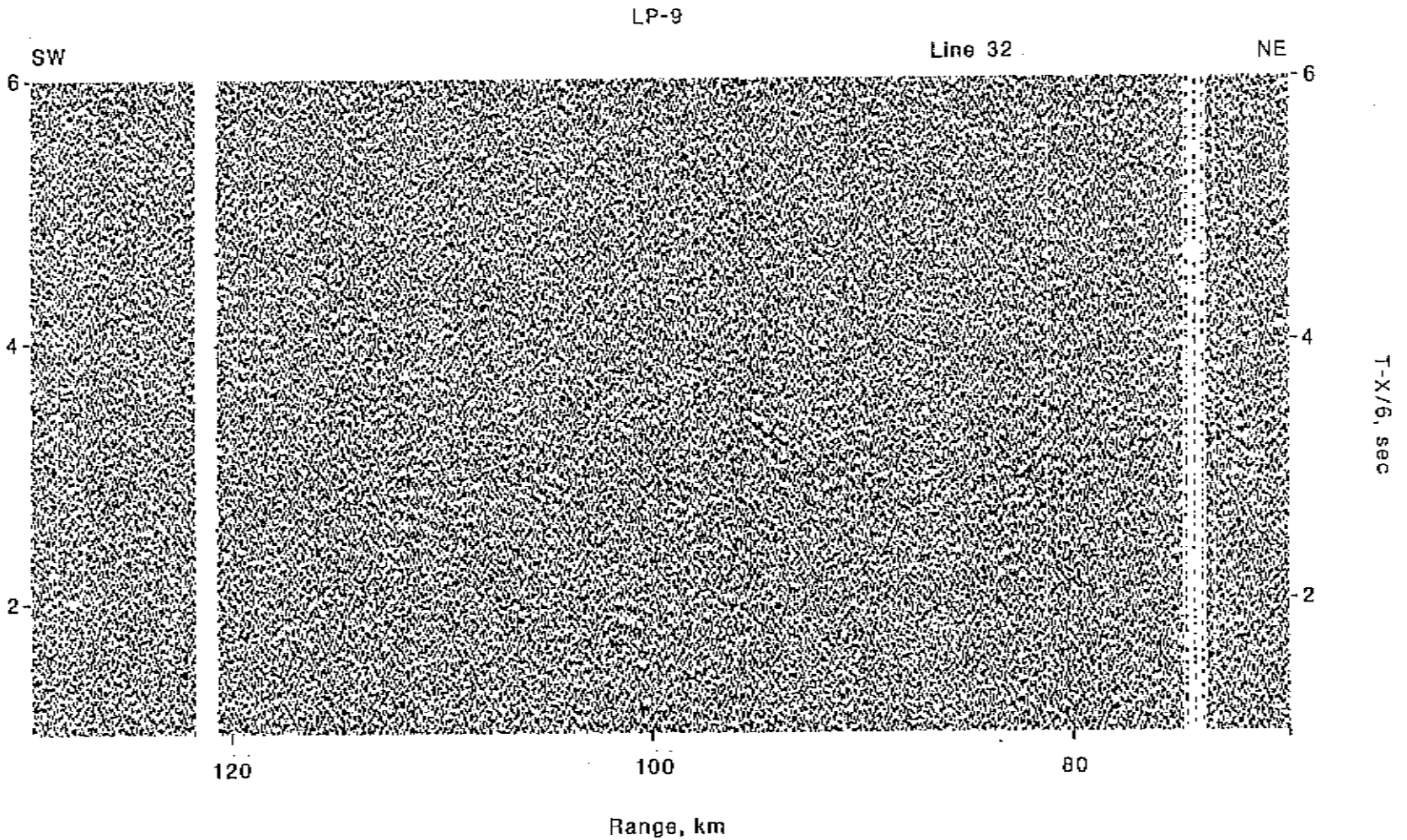

FIGURE 24. Receiver gather LP-9 from line 32. The record section has been linearly reduced using a velocity of 6 km/s and trace amplitudes have been scaled according to Range$^{0.7}$. A few noisy traces have been deleted.

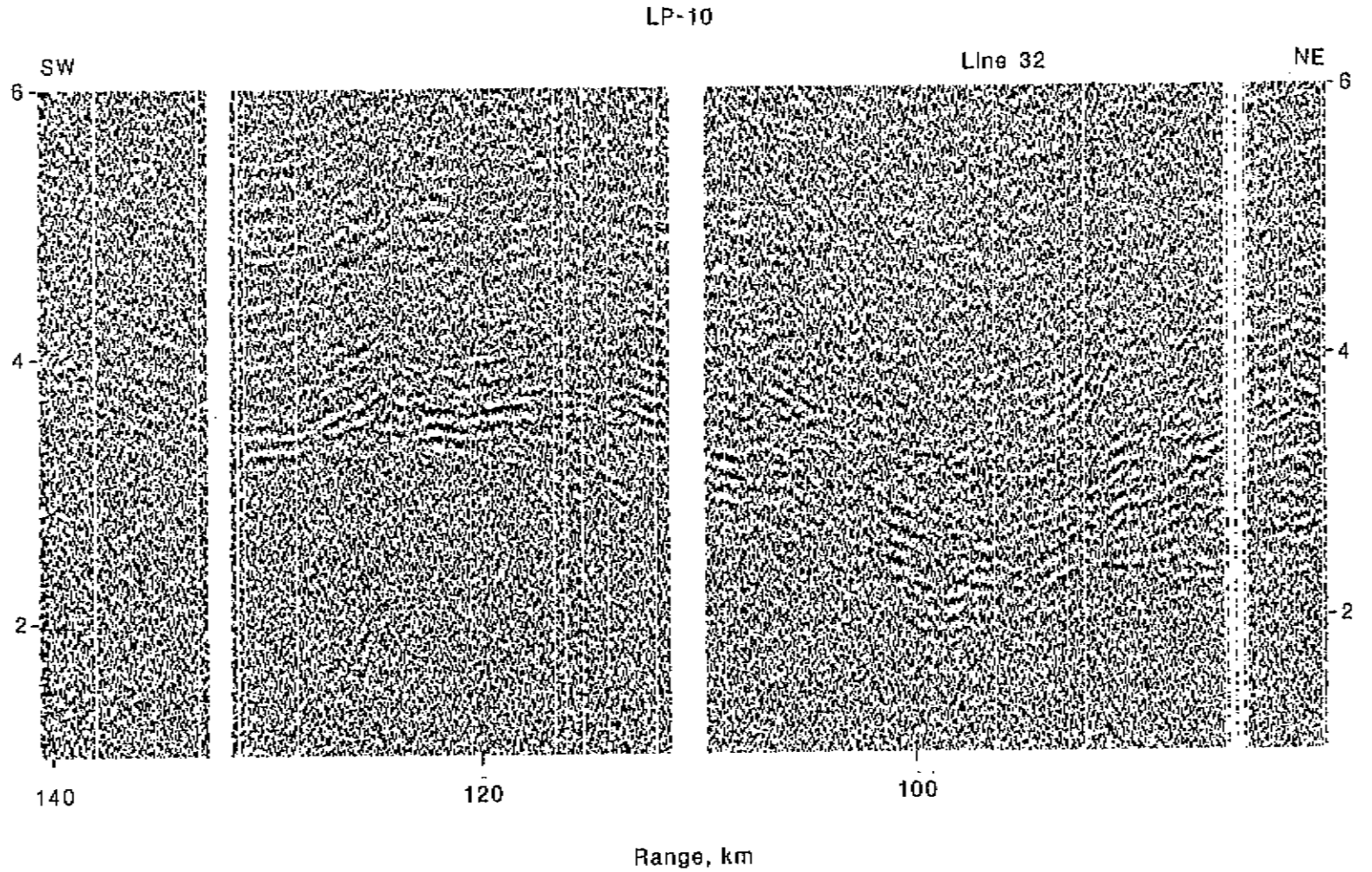

FIGURE 25. Receiver gather recorded at Station LP-10 for line 32. The record section has been deconvolved, linearly reduced using a velocity of 6 km/s, and trace amplitudes have been scaled according to Range$^{0.7}$. A few noisy traces have been deleted.

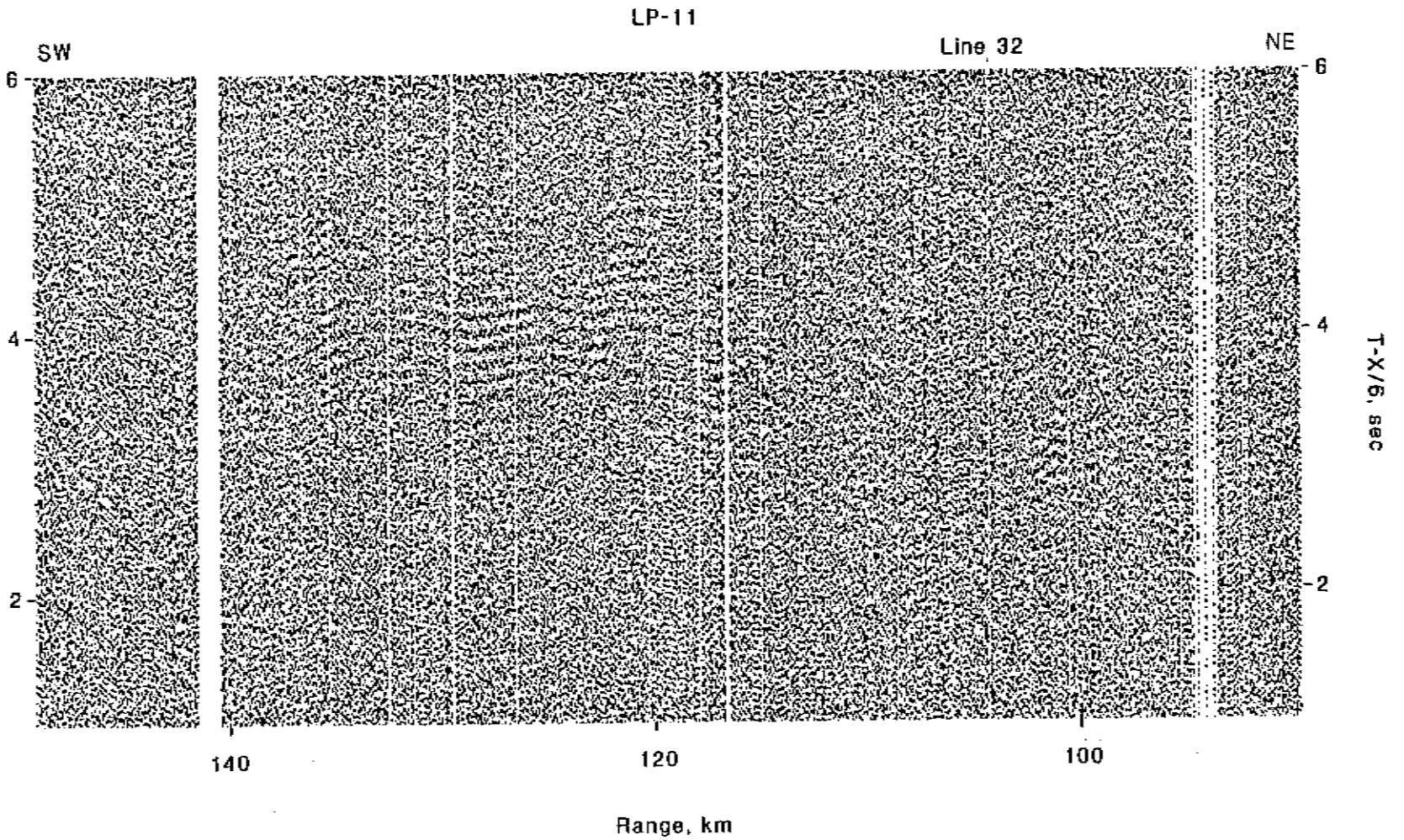

FIGURE 26. Receiver gather LP-11 from line 32. The record section has been linearly reduced using a velocity of 6 km/s and trace amplitudes have been scaled according to Range$^{0.7}$. A few noisy traces have been deleted.

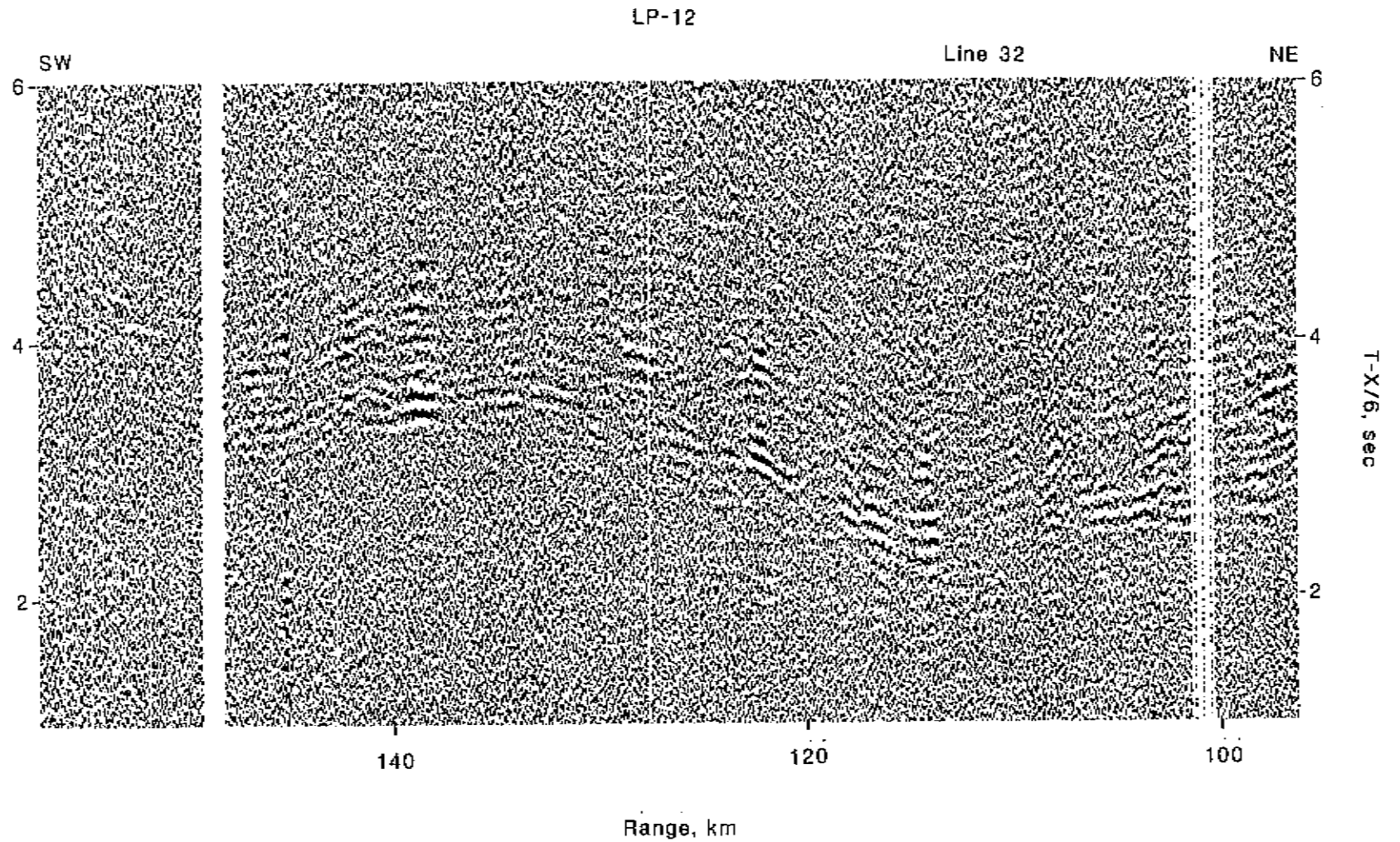

FIGURE 27. Receiver gather LP-12 from line 32. The record section has been linearly reduced using a velocity of 6 km/s and trace amplitudes have been scaled according to Range$^{0.7}$. A few noisy traces have been deleted.

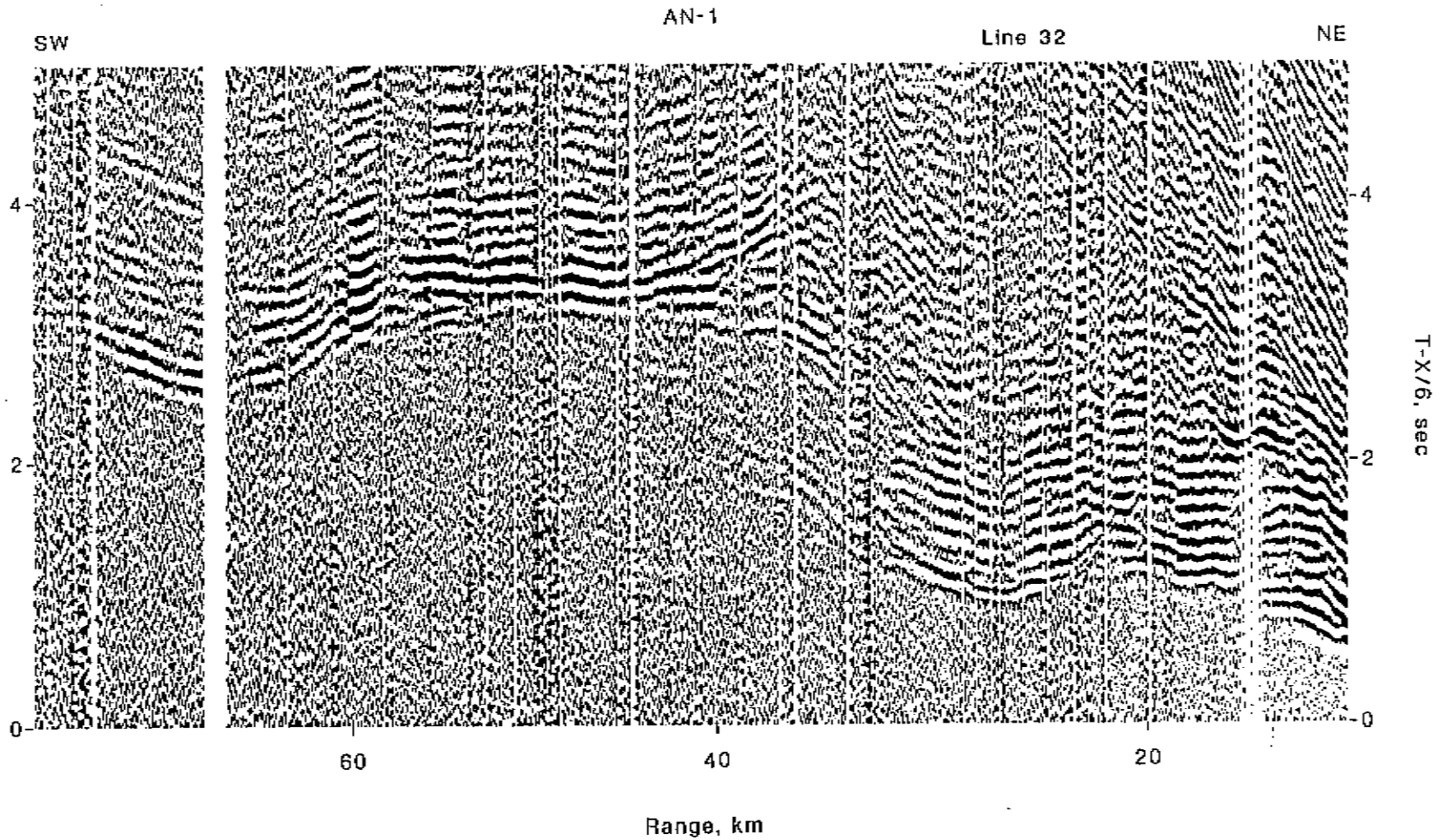

FIGURE 28. Receiver gather AN-1 from line 32. The record section has been linearly reduced using a velocity of 6 km/s and trace amplitudes have been scaled according to Range$^{0.7}$. A few noisy traces have been deleted.

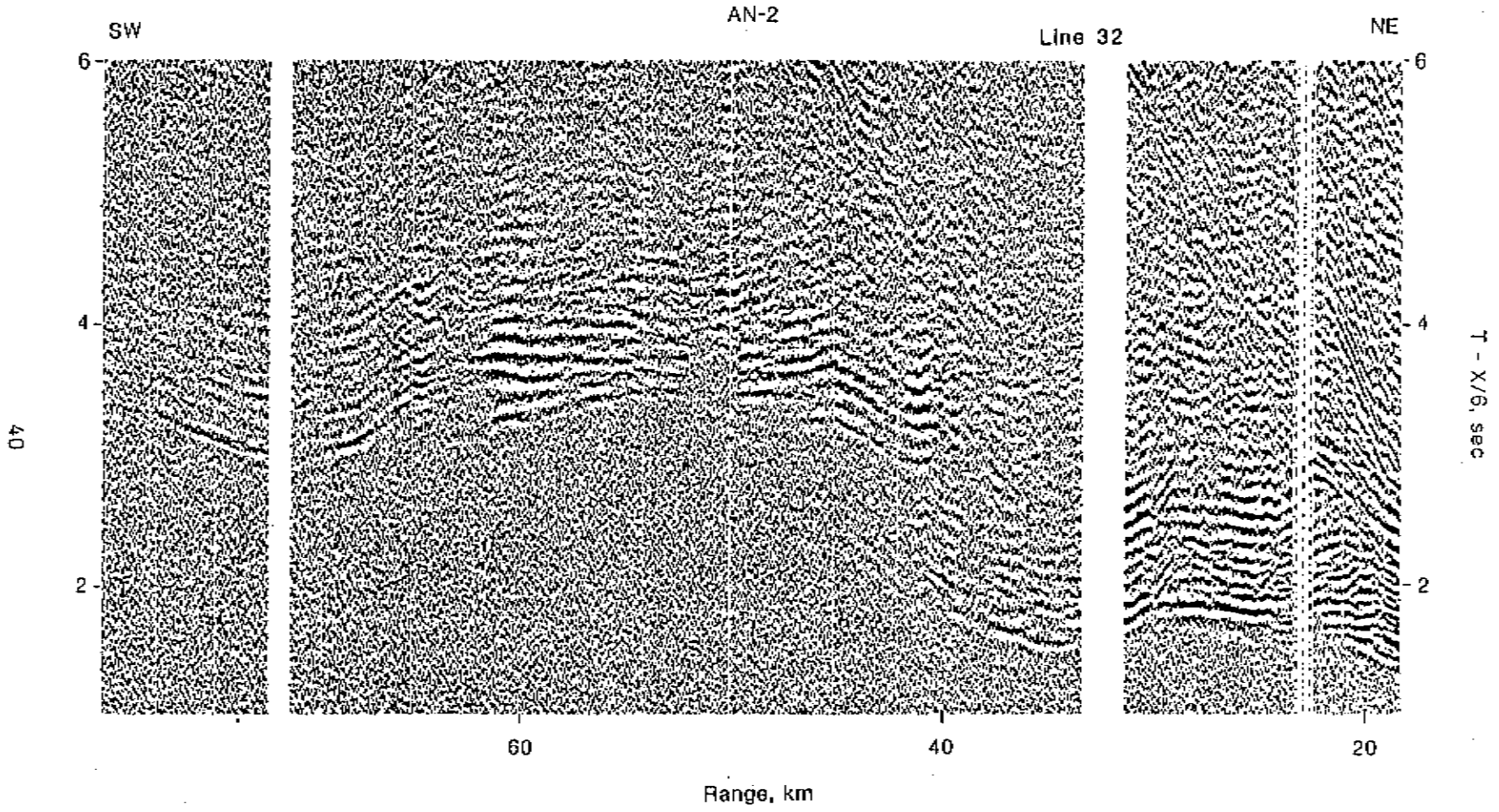

FIGURE 29. Receiver gather AN-2 from line 32. The record section has been linearly reduced using a velocity of 6 km/s and trace amplitudes have been scaled according to Range$^{0.7}$. A few noisy traces have been deleted.

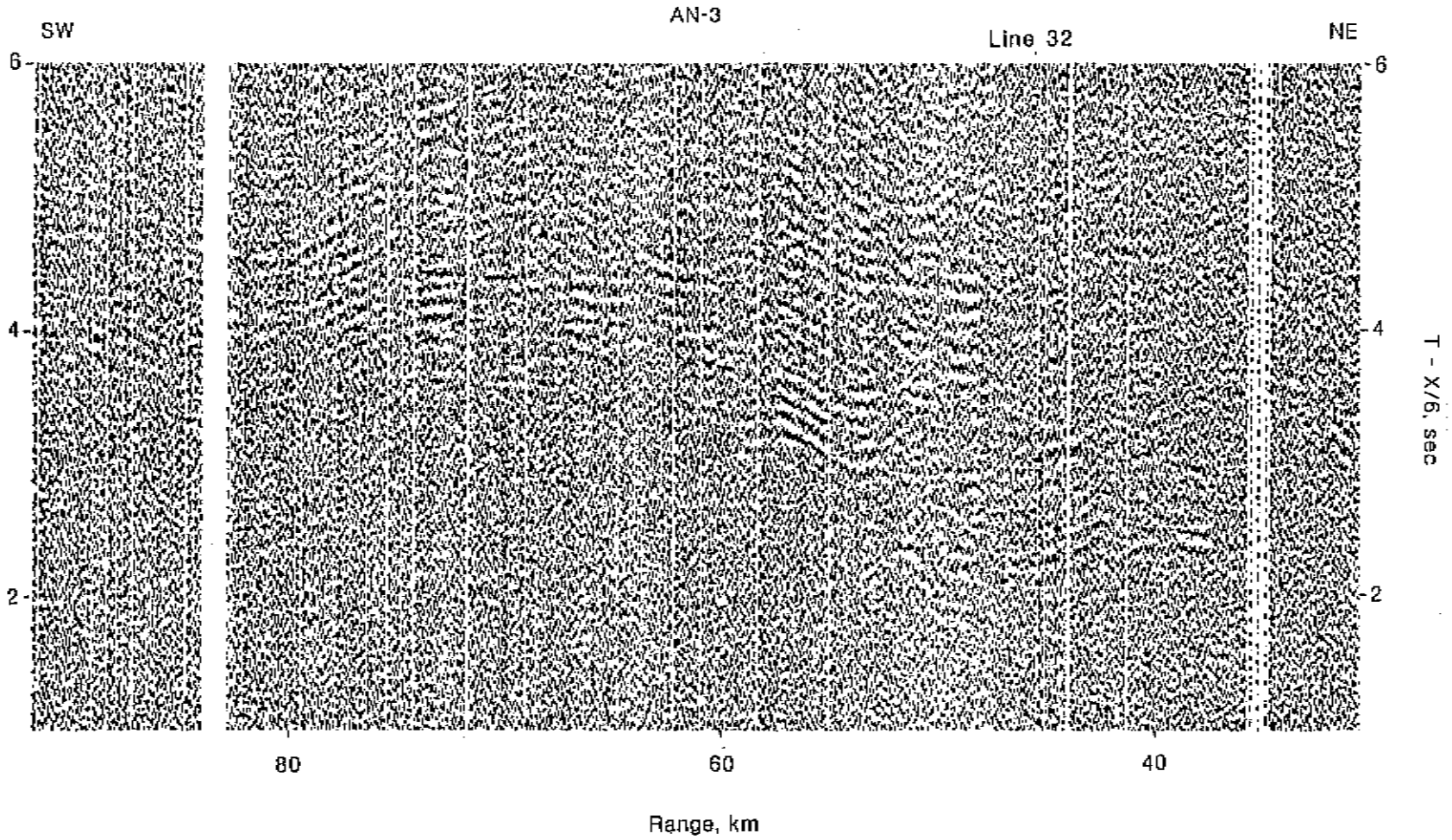

FIGURE 30. Receiver gather AN-3 from line 32. The record section has been linearly reduced using a velocity of 6 km/s. Trace amplitudes have been scaled according to Range$^{0.7}$. A few noisy traces have been deleted.

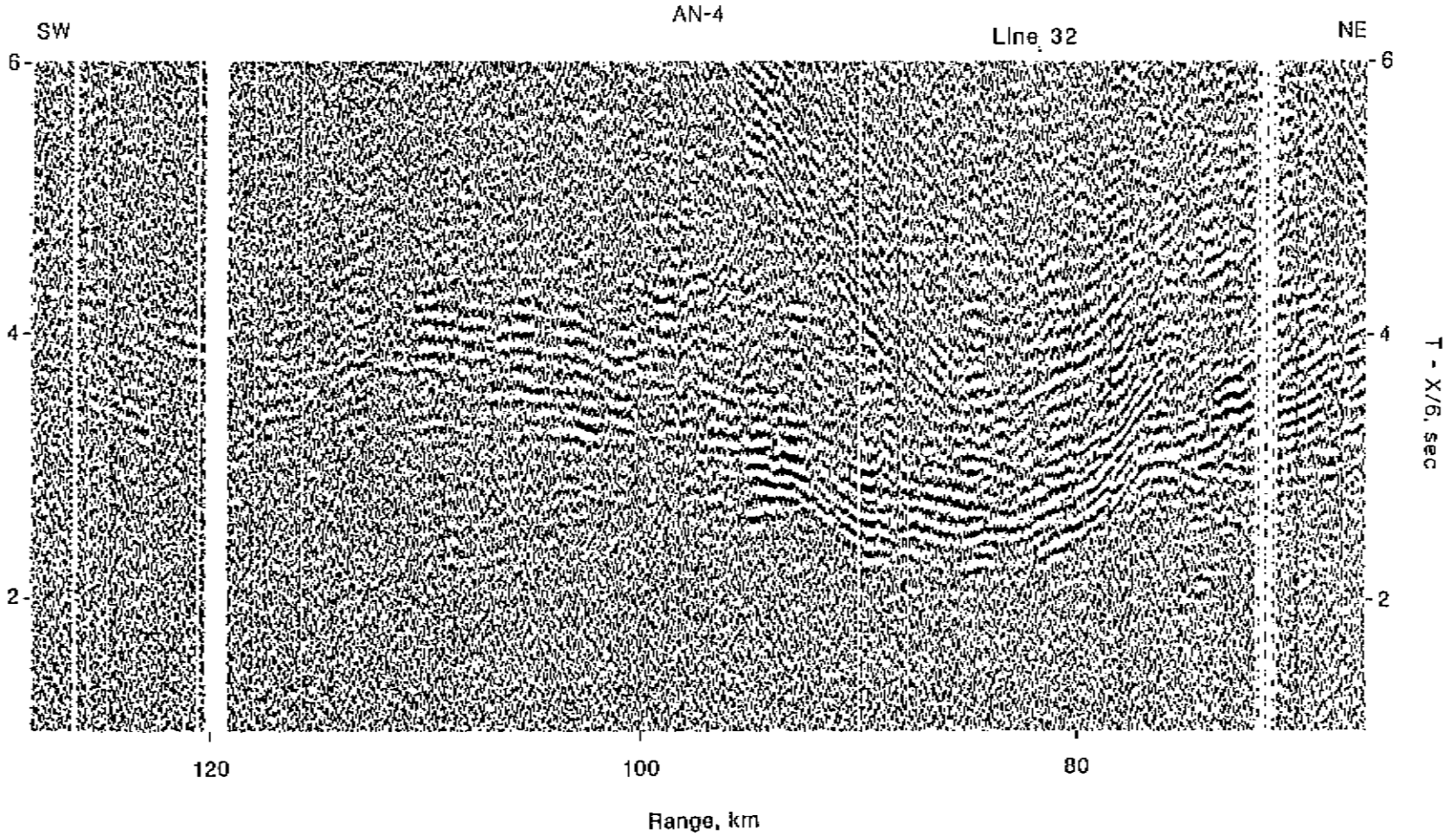

FIGURE 31. Receiver gather AN-4 from line 32. The record section has been linearly reduced using a velocity of 6 km/s and trace amplitudes have been scaled according to Range$^{0.7}$. A few noisy traces have been deleted.

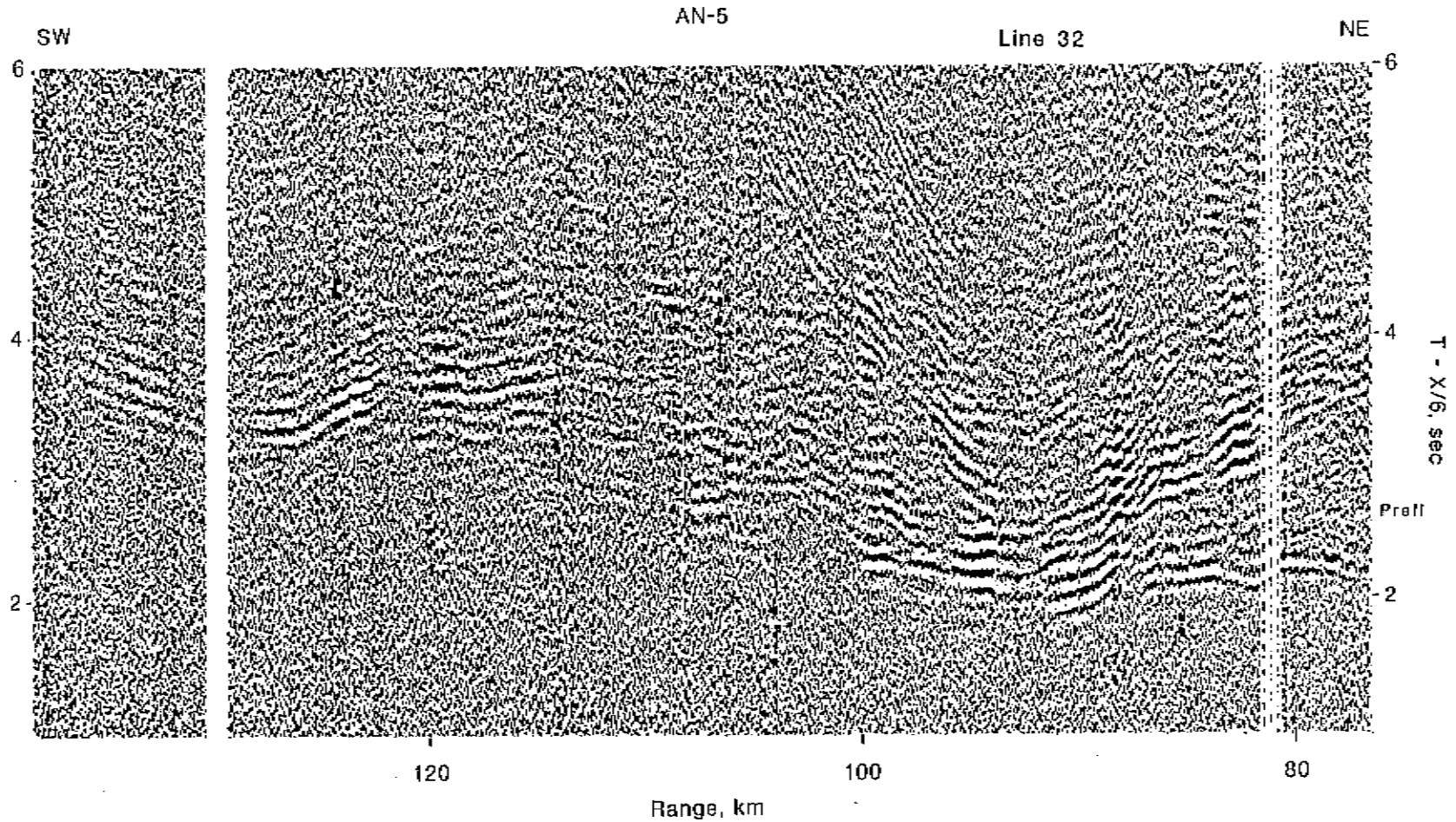

FIGURE 32. Receiver gather AN-5 from line 32. The record section has been linearly reduced using a velocity of 6 km/s and trace amplitudes have been scaled according to Range$^{0.7}$. A few noisy traces have been deleted.

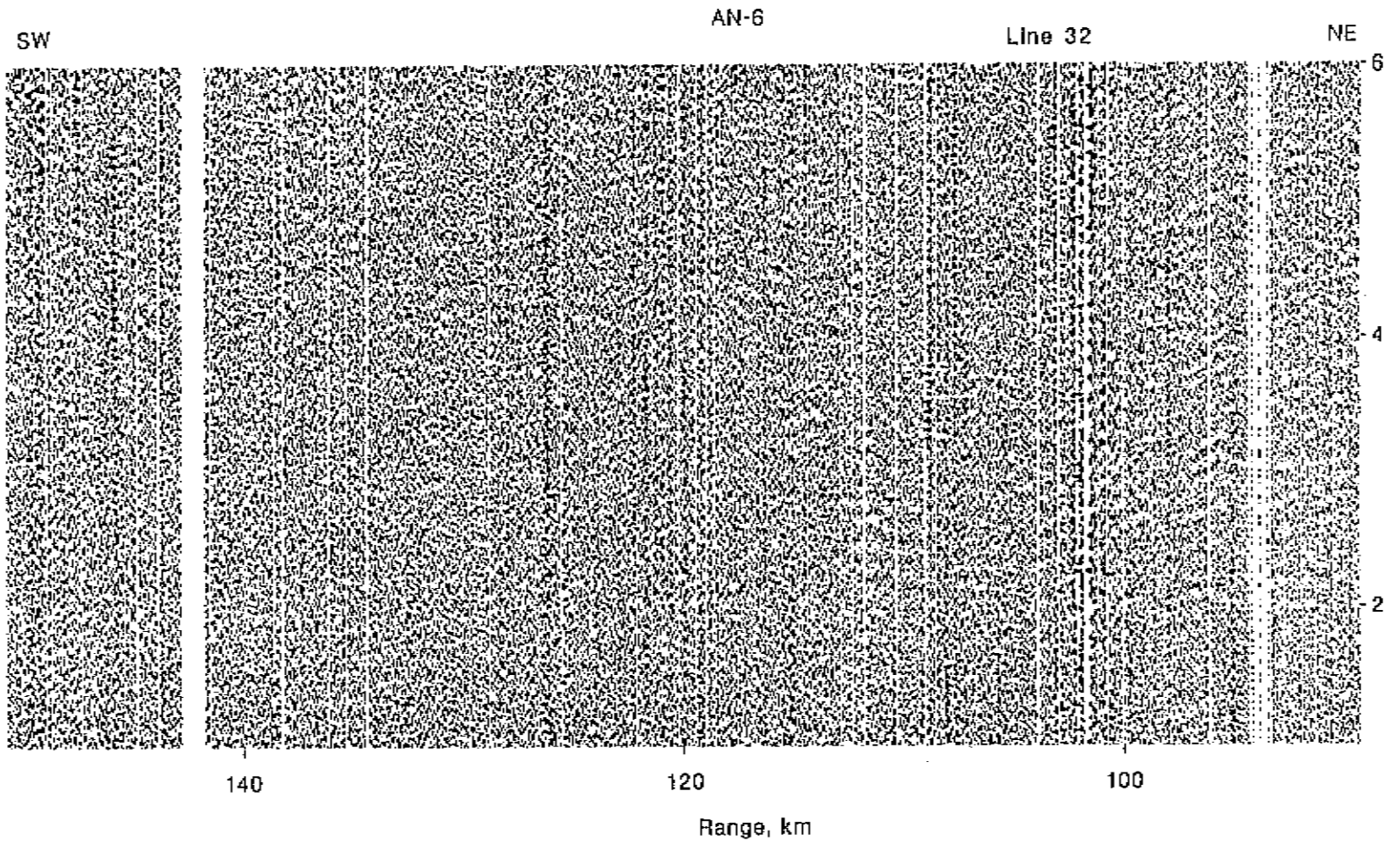

FIGURE 33. Receiver gather AN-6 from line 32. The record section has been linearly reduced using a velocity of 6 km/s. Trace amplitudes have been scaled according to $Range^{0.7}$. A few noisy traces have been deleted.

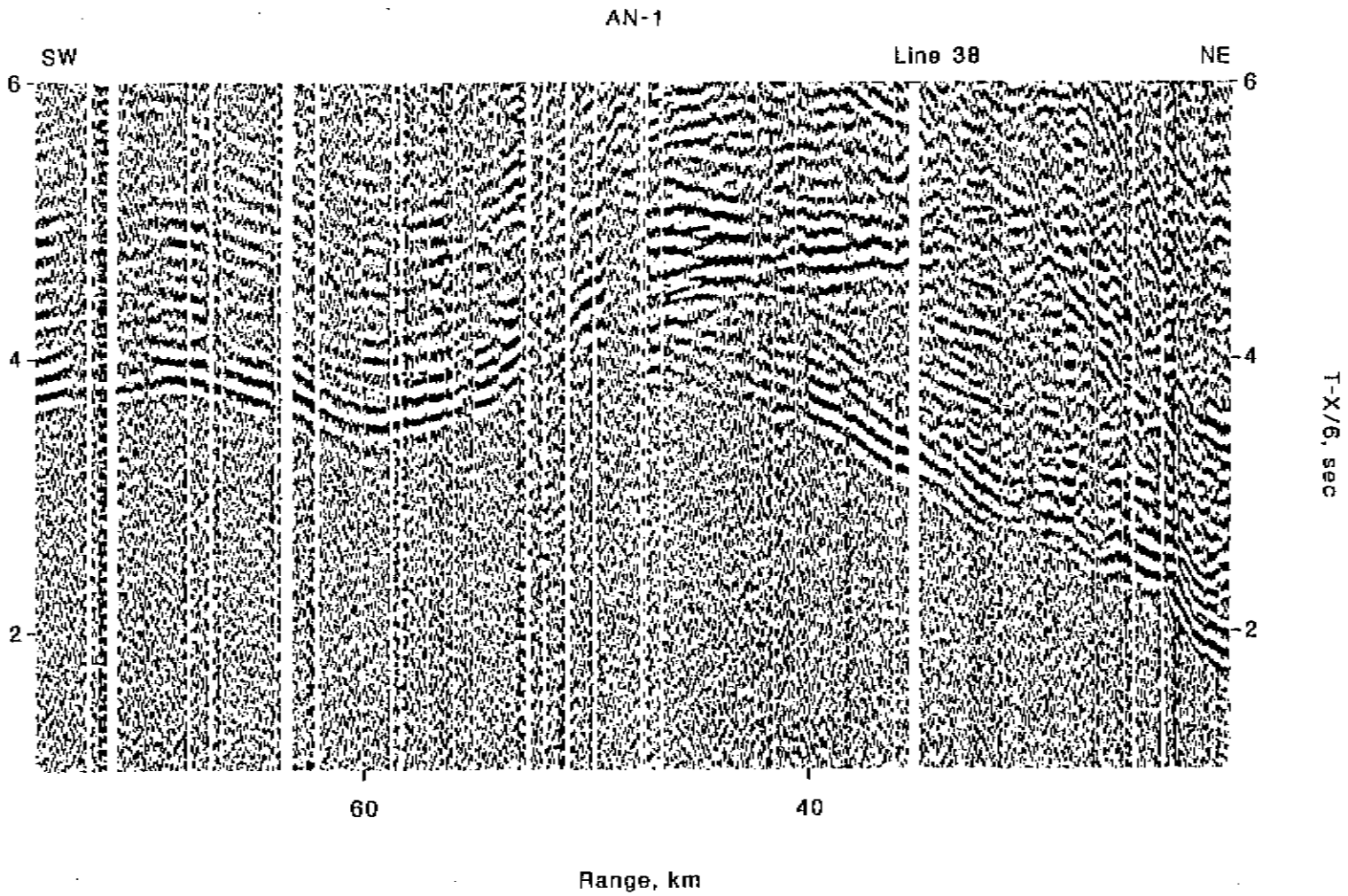

FIGURE 34. Receiver gather AN-1 from line 38. The record section has been linearly reduced using a velocity of 6 km/s and trace amplitudes have been scaled according to Range$^{0.7}$. A few noisy traces have been deleted.

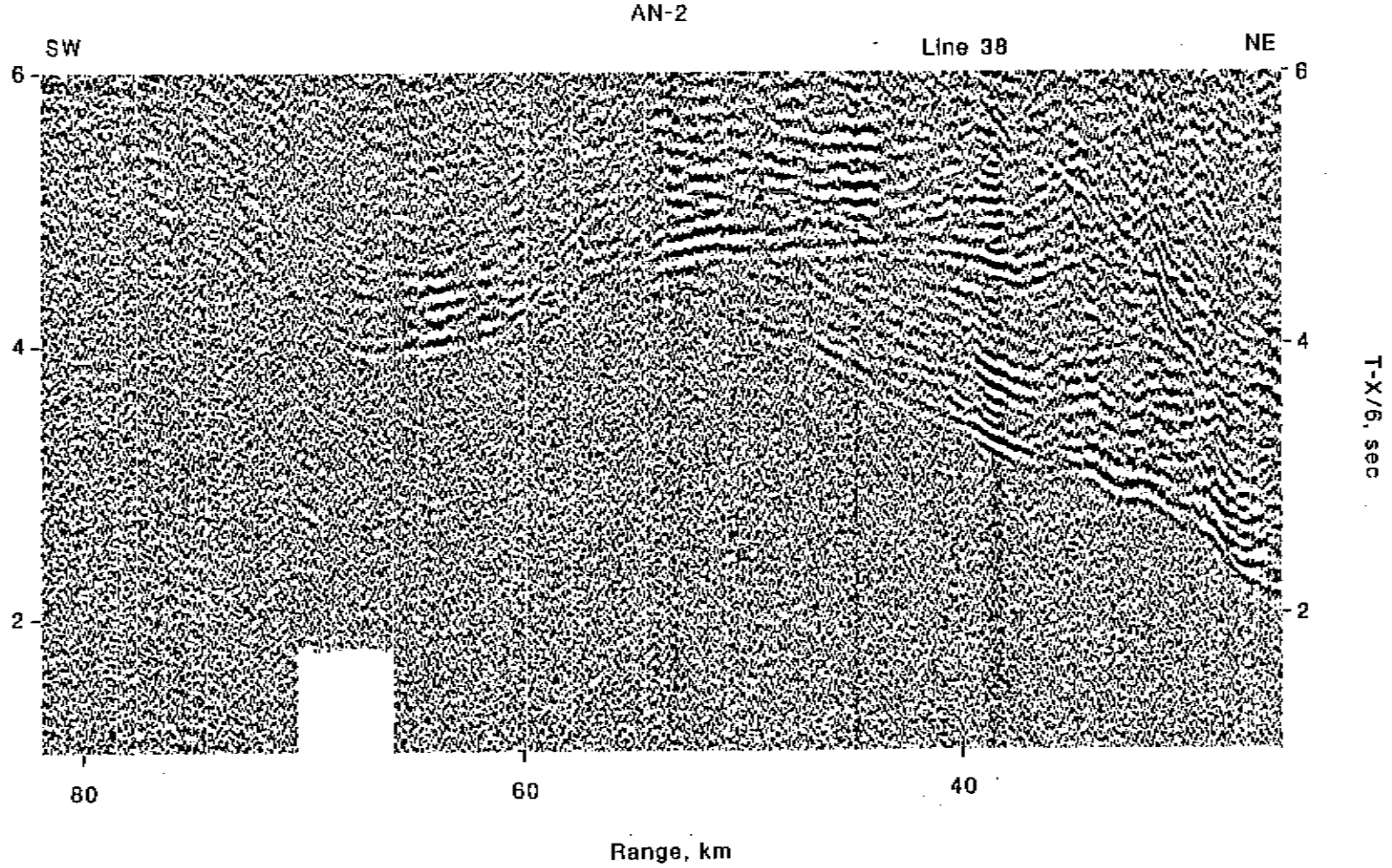

FIGURE 35. Receiver gather AN-2 from line 38. The record section has been linearly reduced using a velocity of 6 km/s and trace amplitudes have been scaled according to Range$^{0.7}$. A few noisy traces have been deleted.

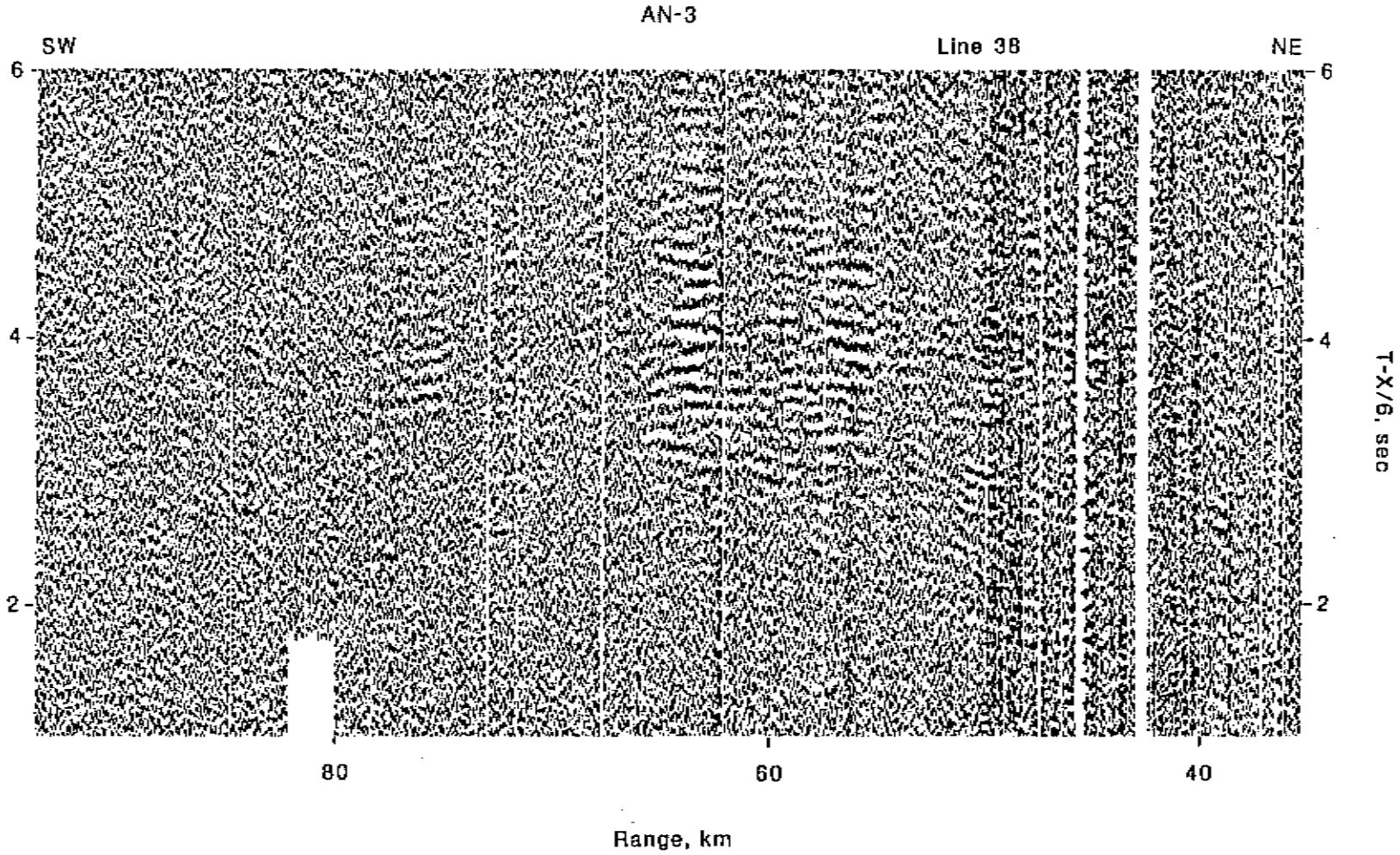

FIGURE 36. Receiver gather AN-3 from line 38. The record section has been linearly reduced using a velocity of 6 km/s and trace amplitudes have been scaled according to Range$^{0.7}$. A few noisy traces have been deleted.

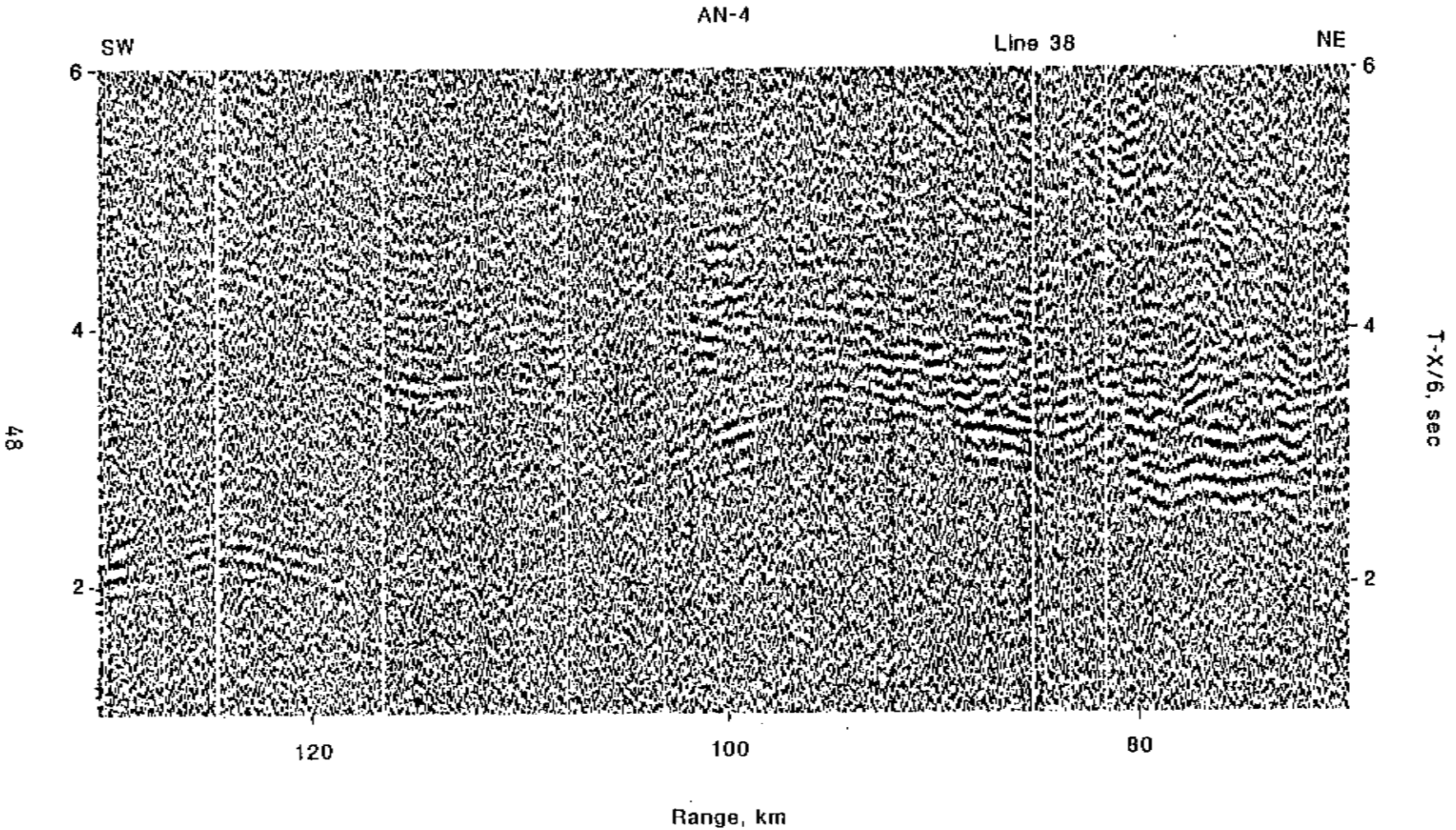

FIGURE 37. Receiver gather AN-4 from line 38. The record section has been linearly reduced using a velocity of 6 km/s and trace amplitudes have been scaled according to Range$^{0.7}$. A few noisy traces have been deleted.

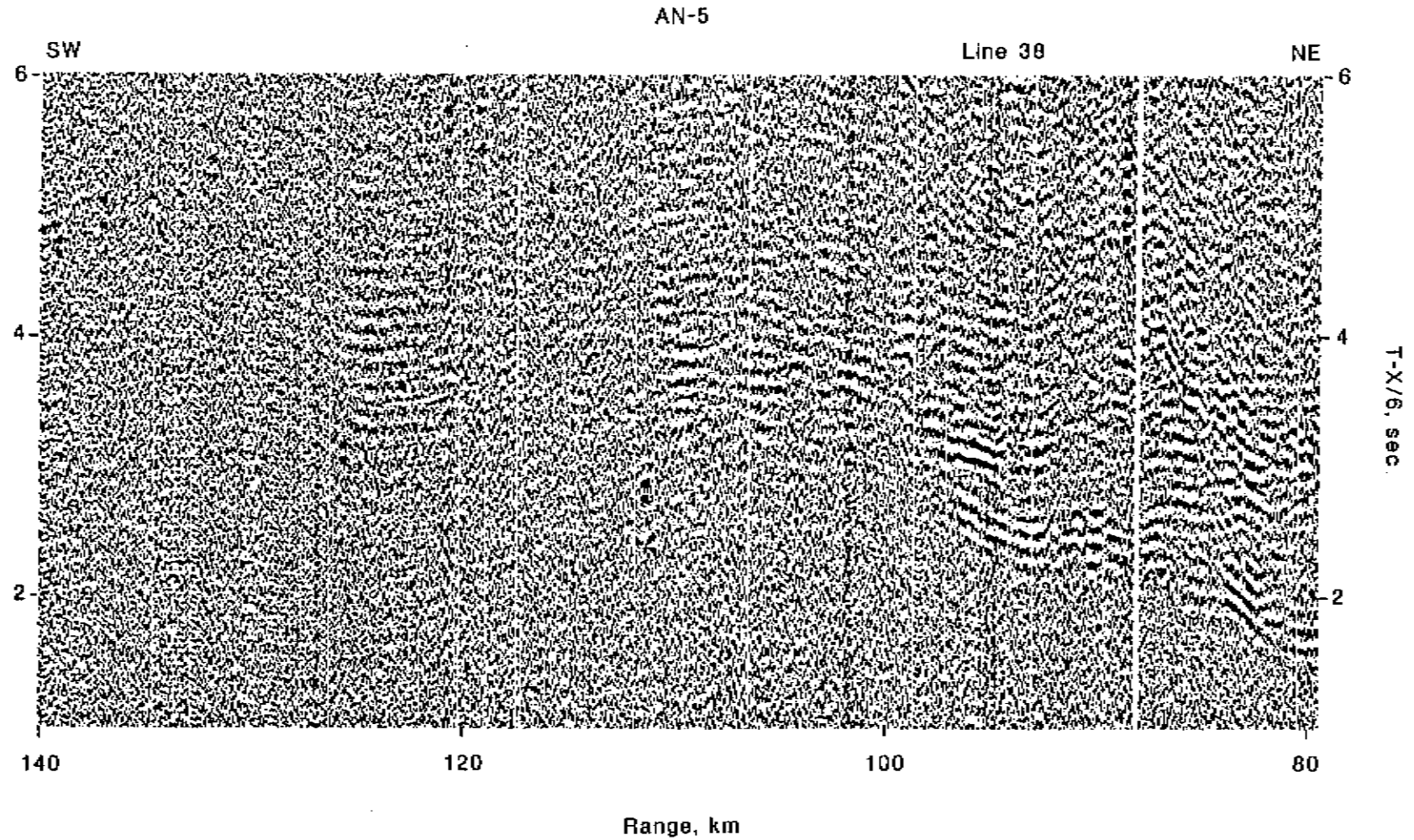

FIGURE 38. Receiver gather AN-5 from line 38. The record section has been linearly reduced using a velocity of 6 km/s and trace amplitudes have been scaled according to Range$^{0.7}$. A few noisy traces have been deleted.

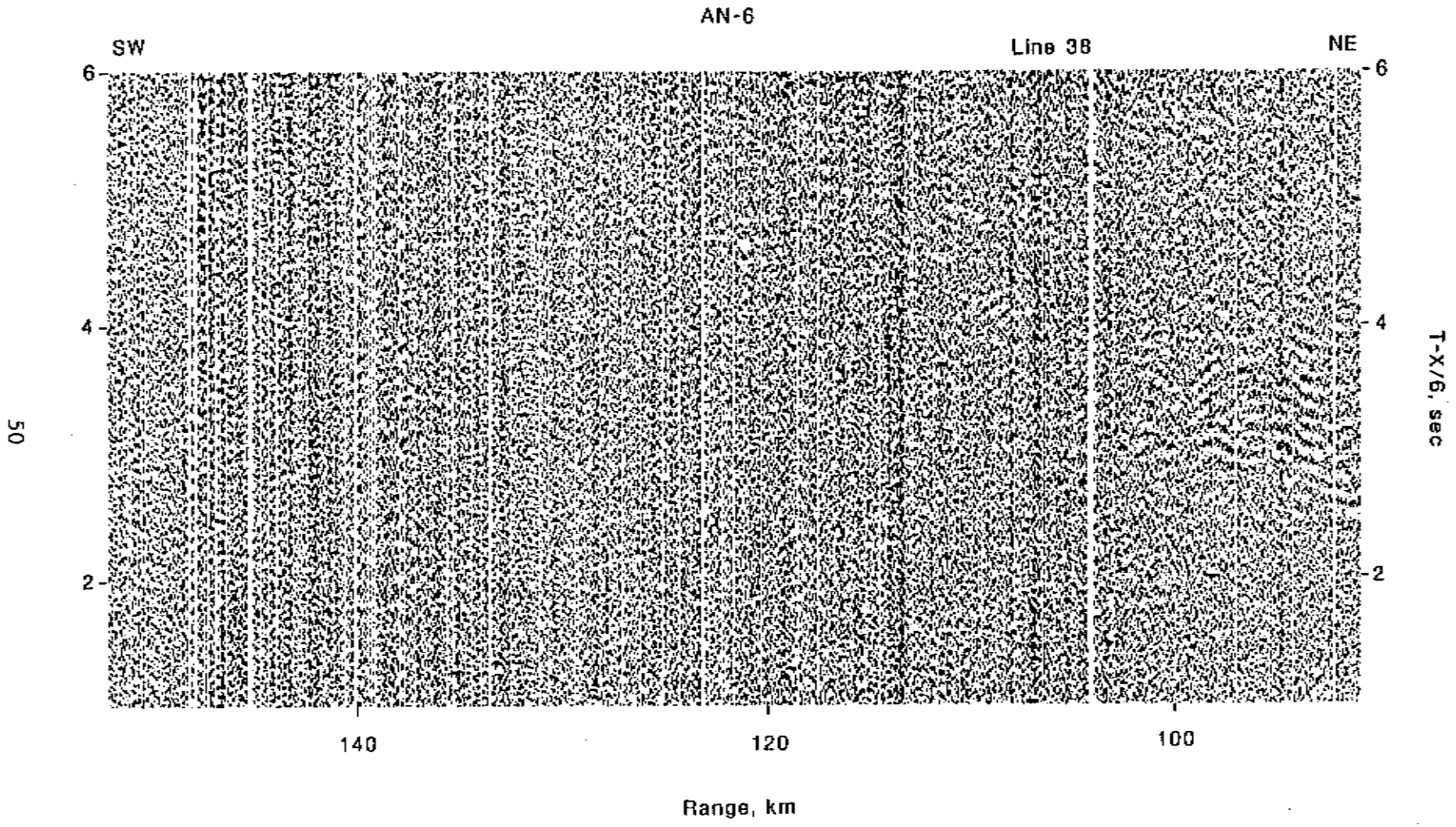

FIGURE 39. Receiver gather AN-6 from line 38. The record section has been linearly reduced using a velocity of 6 km/s and trace amplitudes have been scaled according to Range$^{0.7}$. A few noisy traces have been deleted.

APPENDIX

The following sections summarize the procedures used during the acquisition, digitizing, and processing of the wide-angle data. We focus on those procedures used to constrain shot times and source-receiver offsets.

Data Playback and Digitizing

Because the Motorola PC computer formerly used to digitize five-day tapes (e.g. Brocher and Moses, 1990) became inoperable in 1991, it was replaced by a Everex 386/25 MHz computer with a 386 processor, 4 Mbytes of internal memory, and 300 Mbytes of hard disk memory. This improvement in computer hardware permitted major simplifications and time savings to the processing sequence formerly used to reduce the five-day tapes to seismic record sections.

Using the Compaq Desk Pro 386/25 we digitized data from the five-day data at 100 samples/sec by running the software program called xdetectv on that computer. The program xdetectv is a version of xdetect, described by Tottingham and Lee (1989). The analog tape drive was manually positioned to the desired time on the tape for the start of digitizing with the aid of an IRIG-C clock code reader; up to 260-minutes-long blocks of analog data were digitized at a time. The digitization of 260 minutes of analog data required approximately 13 minutes of playback time. The digitized data were temporarily stored in Seismic Unified Data System (SUDS) format on the PC clone (Ward and Williams, 1992), then FTP'ed to 2 GByte disk drive on the VAX 11/785, where the data were demultiplexed into two different time code channels and 6 seismometer channels (three low gain channels and three high gain channels).

WWVB time broadcast from Denver, Colorado, in addition to an internal clock code in IRIG-C format, were recorded continuously at each station. Because WWVB time is accurate to a few milliseconds, we preferred to use this clock code to determine the time on the digitized files. When WWVB code could not be used, however, we relied on the internal clock code in IRIG-C

format. As described by Brocher and Moses (1990), the frequently large drift of the internal clock required us to determine and remove the drift rate from comparison to the WWVB code.

Generally, the WWVB clock code was used to determine time on the digitized files. We converted the digitized WWVB clock code to a binary signal. We then filtered this binary code to remove short (1 to 3 samples long) noise pulse in the time code. Our program then read the time of the first minute mark and then counted second marks (where the binary code changes from zero to one) to determine the time within the digitized file. The digitized file was then broken into individual traces for each airgun shot based on the reduced travel time for that receiver using a velocity of 6 km/s. The reduced travel time was calculated from a master list of shot times and locations, the receiver location, and the reduction velocity (normally 6 km/s). 23 seconds of data were saved for each trace. The individual traces were then written in SEG-Y format to a 9-track digital tape.

Most of the software used for this processing sequence was described by Brocher and Moses (1990), and greater available disk space allowed us to merge the several separate software programs described by them into a single program called SUDTOSEGYTEST.FOR. Larger available disk space also allowed us to read the SUDS files from and write the SEG-Y files to the same disk, resulting in considerable time savings relative to the old processing sequence. The record sections were plotted using DISCO Processing Software.

We found that this new processing sequence provided markedly improved seismic sections. In particular, there is very little, if any, timing jitter between traces; the improved phase coherence allows weaker arrivals to be identified and traced to greater ranges. We attribute the improved record quality over that reported by Brocher and Moses (1990) to the improved method of determining time within the digitized file by counting second marks. As described by Brocher and Moses (1990), the timing within 5-minute-long digitized blocks was accomplished simply by counting samples, after either assuming a digitization interval or determining this interval from half-second marks. This method, however, is limited in accuracy for the first method by the non-constant digitization interval resulting from tape speed fluctuations during playback and for the

second method by noise spikes in the time code. The new algorithm used here appears to provide a more accurate timing and markedly improves the quality of the seismic data.

Recorder Locations and Elevations

The locations and elevations of the five-day recorders summarized in Table 1 were obtained using GPS receivers operated in differential mode. These receiver locations and elevations are estimated to be accurate to within several meters.

Recorder Times of Operations

The five-day recorders and transmitter stations were deployed over a period of time lasting several days and were then turned on prior to the acquisition of seismic reflection lines 32 and 38. Table 3 therefore provides a listing of the times for which each five-day recorder actually recorded data.

TABLE 3. 5-day Recorder Times of Operation

Site No.	Name	Time On JD Hr. Min.	Time Off JD Hr.Min.
LP-1*	Majors Creek	120 1720	127 0445
LP-2	Empire Grade	120 1720	127 0445
LP-3	Happy Valley	120 1852	127 0615
LP-4	Olive Springs	120 0155	126 1430
LP-5	Loma Prieta	120 0013	126 1115
LP-6	Casa Loma Rd.	120 0045	126 1330
LP-7	Bailey Rd.	119 2307	126 1100
LP-8	Coe Ranch	120 0427	126 1615
LP-9*	San Felipe Rch.	120 0427	126 1615
LP-10	Arnold Ranch	118 0424	>129 0000
LP-11*	Red Mtn.	119 0020	125 1600
LP-12	Arkansas Cyn.	119 0020	125 1600
LP-13	Ingram Cyn.	119 0400	>129 0000

TABLE 3 Continued.

Site No.	Name	Time On JD Hr. Min.	Time Off JD Hr.Min.
AN-1	Waddell Creek	120 1525	127 0330
AN-2*	Eagle Creek	119 2141	126 1000
AN-3	Mt. Bielawski	119 2141	126 1000
AN-4	Calaveras Res.	121 0404	128 1415
AN-5	Valpe Ridge	120 2212	127 1000
AN-6	Mines Road	123 0508	>129 0000

*Transmitter Station consisting of vertical component seismometer only.

Operations on the R/V S.P. Lee

From April 24, 1990 (Julian Day 114) until May 8, 1990 (Julian Day 128), the R/V **S.P. Lee** acquired a total of 62 seismic reflection profiles from just north of Bodega Bay to just south of Monterey (Lewis, 1990). Most of the seismic lines were oriented perpendicular to the coastline and margin, although several strike lines parallel to the coast were also obtained. Of the 62 reflection profiles acquired, elements of the temporary five-day seismograph array recorded profiles 12-62, extending from the latitudes of Bolinas to Monterey. In Table 4 we provide detailed information for selected reflection lines near the five-day recorder array.

TABLE 4. R/V **S.P. Lee** Airgun Firing Times and Locations

GMT Begin JD HRMIN	Lat. (N) Deg. Min.	Long. (W) Deg. Min.	GMT End JD HRMIN	Lat. (N) Deg. Min.	Long. (W) Deg. Min.
		Line 12			
117 1940	37 47.16	122 42.41	118 0520	37 18.59	123 31.83
		Line 13			
118 0705	37 15.56	123 24.24	118 1545	37 38.01	122 38.47
		Line 14			
118 1656	37 34.67	122 36.97	118 2239	37 19.54	123 07.65
		Line 17			
119 0909	37 10.30	122 34.52	119 1235	36 56.20	122 16.84
		Line 27			
122 0825	37 23.81	122 33.60	122 1903	36 57.25	123 28.13
		Line 28			
122 2040	36 51.84	123 24.94	123 0157	37 16.84	122 31.51

TABLE 4 continued.

GMT Begin JD HRMIN	Lat. (N) Deg. Min.	Long. (W) Deg. Min.	GMT End JD HRMIN	Lat. (N) Deg. Min.	Long. (W) Deg. Min.
		Line 31			
123 1527	36 53.35	122 30.80	123 2017	36 39.82	122 49.54
		Line 32			
123 2113	36 41.80	122 52.43	124 0330	37 3.40	122 21.35
		Line 38			
124 1849	36 55.25	122 13.22	125 0155	36 33.42	122 44.27
		Line 39			
125 0254	36 30.29	122 41.94	125 1107	36 52.19	122 00.00

Shot Instant Timing

Shot instant times of the airgun array were obtained from "start of recording cycle" times recorded on the R/V **S.P. Lee.** "Start of recording cycle" times represent the leading edge of an electrical square wave used to start the magnetic tape drives for recording the multichannel streamer data and to trigger the airgun array. These times were recorded in the header of the multichannel seismic reflection data obtained from the resulting airgun signal. A Kinemetrics True Time satellite clock receiver (model 468), set for the local time delay to the GOES satellite, and stabilized using a

high-precision Cesium oscillator, provided the absolute time base recorded on the R/V **S.P. Lee**. The GOES clock receiver produces time accurate to a millisecond, and within this precision produces time identical to the time produced by the OMEGA Clock Receiver used onshore as a "master" clock for the five-day recorders. The "start of recording cycle times" were recovered when the data were demultiplexed at the DISCO data processing center, and were merged into one computer file per seismic line.

Shot instant times were calculated from the "start of recording cycle" times using the following algorithm. To conserve magnetic tape on the **S.P. Lee**, a variable recording delay, called the deep-water delay, was applied depending on the water depth. In shallow water when a deep-water-delay of 0 seconds was applied, i.e., no delay was applied, 3.227 seconds were added to the "start of recording cycle" times to obtain shot instant times. When a deep-water-delay of 1 second was applied, 2.227 seconds were added to the "start of recording cycle" time. When a deep-water-delay of 2 seconds was applied, 1.227 seconds were added to the "start of recording cycle" times to obtain shot instant times.

We observed that the origin times of a few shots were not properly corrected following the above algorithm. We therefore adjusted these times by increments of 0.5 and 1.0 s to match the arrival times of adjacent shots. While we cannot explain these anomalous times, we believe that these unaccounted time shifts were caused by use of erroneous deep-water-delays during the acquisition of the reflection data; these delays would neither effect nor be detected in the processing of the reflection data.

Navigation

Navigation onboard the R/V **S.P. Lee** was accomplished using Loran-C navigation occasionally corrected by GPS locations. The rho-rho Loran-C navigation was updated by a GPS receiver operated in selected availability mode, resulting in an estimated accuracy of 150 to 200 m.

Factors Influencing Data Quality

Data quality was highest for stations near the coast closest to the reflection lines (LP-1 through LP-5 and AN-1 through AN-2), and generally decreased as the distance of the station from the coast increased. Data quality was also reasonable at some of the remote recorder locations within the Santa Cruz Mountains (LP 10 and LP-12) and the Diablo Range (AN-4 through AN-5) (fig. 1), where the seismometers were deployed on or near outcrops of basement rocks (Table 5). Sites LP-9, LP-11, LP-13, AN-3, and AN-6 produced marginal to poor quality data. Amplifier gains were set too low at Stations LP-9 and LP-11, which degraded the data quality from those stations. Data quality was degraded at sites near heavily traveled highways: LP-7 was sited near State Highway 101, and LP-13 was sited near Interstate Freeway 5.

TABLE 5. Types of Seismometer Plants

Site No.	Name	Seismometer Plant Description
LP-1	Majors Creek	Weathered sandstone bedrock
LP-2	Empire Grade	Weathered sandstone bedrock
LP-3	Happy Valley	Weathered sandstone bedrock
LP-4	Olive Springs	Weathered sandstone bedrock
LP-5	Loma Prieta	Weathered metasediment bedrock
LP-6	Casa Loma Rd.	Weathered metasediment bedrock
LP-7	Bailey Rd.	Weathered metasediment bedrock
LP-8	Coe Ranch	Soil above metasediment bedrock
LP-9	San Felipe Rch.	Weathered metasediment bedrock
LP-10	Arnold Ranch	Weathered metasediment bedrock
LP-11	Red Mtn.	Weathered metasediment bedrock
LP-12	Arkansas Cyn.	Weathered metasediment bedrock
LP-13	Ingram Cyn.	Weathered metasediment bedrock
AN-1	Waddell Creek	Weathered sandstone/chert bedrock
AN-2	Eagle Creek	Granitic bedrock
AN-3	Mt. Bielawski	Weathered sandstone bedrock
AN-4	Calaveras Res.	Weathered metasediment bedrock
AN-5	Valpe Ridge	Weathered metasediment bedrock
AN-6	Mines Road	Weathered metasediment bedrock

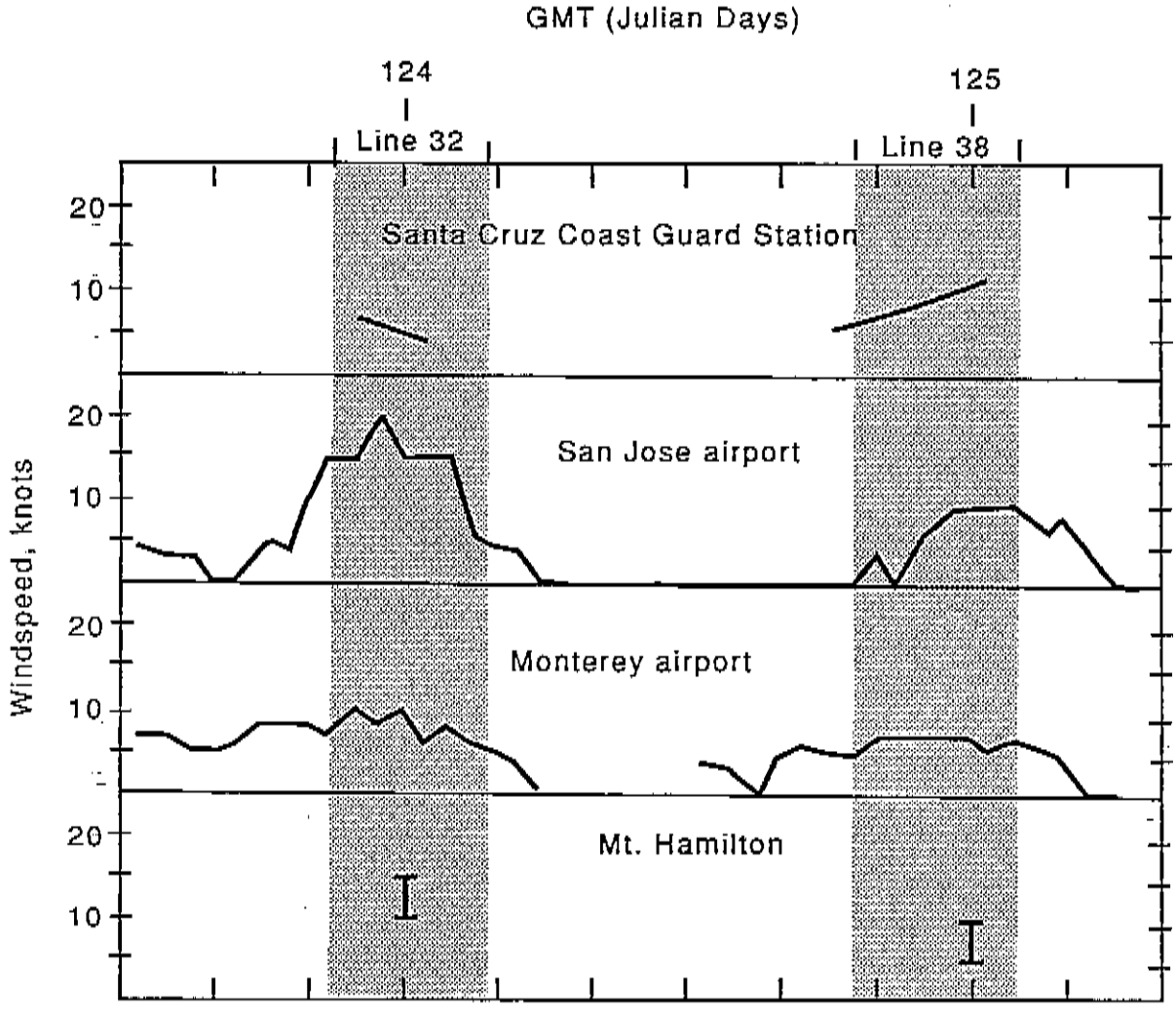

FIGURE 40. Comparison of windspeed (in knots) versus time during the acquisition of lines 32 and 38 at four different locations near the seismic arrays. Shaded times indicate the time periods during which airgun signals from line 32 and 38 were recorded.

Ambient wind speeds during our experiment were relatively high, significantly raising seismic noise levels. Windspeed records from Santa Cruz airport show higher winds for Line 38 than for Line 32, suggesting that the higher data quality recorded during Line 32 versus Line 38 is atributable to lower average windspeeds when Line 32 was obtained (compare recordings at LP stations obtained from Lines 32 and 38 in Figures 3-15 and 16-27). Windspeed records from other Bay Area airports (San Jose, Monterey) and Mt. Hamilton, however, do not support this inference (fig. 40). Therefore, it is also possible that the airgun array functioned better during Line 32 than during Line 38.

The recording of lines 32 and 38 during daylight hours also contributed to the lowered signal-to-noise ratios of the data. Previous experience in refraction profiling demonstrates that in areas of high population density, data quality would have been improved by recording the wide-angle profiles at night. The windspeed data in Figure 40 also suggest that data quality would have been improved had the data been recorded at night.

SEG-Y Tape Format

The wide-angle seismic reflection/refraction profiles obtained by these procedures were written to 9-track tapes in SEG-Y format. Three traces were written for each shot and receiver pair; trace 1 contains the high gain N/S horizontal seismometer component. Trace 2 contains the high-gain vertical seismometer component and Trace 3 contains the high-gain E/W horizontal seismometer component. Each trace contains a 240-byte trace header of 2- and 4-byte integers describing the specific trace and 2301 2-byte integer data samples. The location of each value in the SEG-Y trace header as described by Barry and others (1975) was slightly modified as described by Luetgert and others (1990). All trace integer values were byte swapped from DEC to SEGY-IBM format and are written in SEGY-IBM16INT format. An End of Tape (EOT) mark was written at the end of each 12-inch, 6250 BPI, SEG-Y tape.

ACKNOWLEDGEMENTS

Numerous private landowners kindly gave us permission to locate 5-day recorders on their property. Mr. Kevin Shea of East Bay Regional Park District and Chief Lucky of the California Department of Forestry provided access to property under their jurisdiction. John Coakley and others of the USGS-Menlo Park deployed the 5-day recorders. Will Kohler provided programming assistance. Steve Hughes, Steve Larkin, and Jill McCarthy helped us transfer the 5-day recorder data into SEG-Y format. Dennis Mann and Jon Childs shared information on the seismic reflection profiling onboard the R/V **S.P. Lee**. Stephen Hughes provided useful comments on an earlier draft of this report.

This work was supported by the National Earthquake Hazards Reduction and the Offshore Geologic Framework Programs.

REFERENCES CITED

Barry, K.M., D.A. Cravers, and C.W. Kneale, 1975, Recommended standards for digital tape formats: *Geophysics, v. 40*, p. 344-352.

Brocher, T.M., and M.J. Moses, 1990, Wide-angle seismic recordings obtained during the TACT multichannel reflection profiling in the northern Gulf of Alaska: *U.S. Geological Survey, Open-file Report 90-663*, 40 pp.

Brocher, T.M., M. J. Moses, and S. D. Lewis, 1991, Crustal structure of the continental margin and San Andreas fault in the vicinity of Loma Prieta based on onshore-offshore wide-angle seismic profiling, *EOS, Transactions of the American Geophysical Union, v. 72*, p. 328.

Clark, D.H., N.T. Hall, D.H. Hamilton, and R.G. Heck, 1991, Structural analysis of late Neogene deformation in the central offshore Santa Maria basin, California: *Journal of Geophysical Research, v. 96*, p. 6435-6457.

Criley, E., and J. Eaton, 1978, Five-day recorder seismic system: *U.S. Geological Survey Open-file Report 78-266*, 85 pp.

Curray, J.R., 1966, Geologic structure on the continental margin, from subbottom profiles, northern and central California: *California Division of Mines and Geology, Bulletin 190*, p. 337-342.

Dickinson, W.R., 1970, Relations of andesites, granites, and derivative sandstones to arc-trench tectonics: *Reviews of Geophysics, v. 8*, p. 813-860.

Ernst, W.G., 1971, Do mineral parageneses reflect unusually high-pressure conditions of Franciscan metamorphism?: *American Journal of Science, v. 270*, p. 81-108.

Ewing, J., and M. Talwani, 1991, Marine deep seismic reflection profiles off central California: *Journal of Geophysical Research, v. 96*, p. 6432-6433.

Lewis, S.D., 1990, Deformation style of shelf sedimentary basins seaward of the San Gregorio fault, central California: *EOS, Transactions of the American Geophysical Union, v. 71*, p. 1631.

Luetgert, J., S. Hughes, J. Cipar, S. Mangino, D. Forsyth, and I. Asudeh, 1990, Data report for O-NYNEX the 1988 Grenville-Appalachian seismic refraction experiment in Ontario, New York, and New England: *U. S. Geological Survey Open-file Report 90-426*, 51 pp.

McCulloch, D.S., 1987, Regional geology and hydrocarbon potential of offshore central California: in Geology and Resource Potential of the continental margin of western North America and adjacent ocean basins - Beaufort Sea to Baja California, edited by D.W. Scholl, A. Grantz, and J.G. Vedder, p. 353-401, *Vol. 6, Circum-Pacific Council for Energy and Mineral Resources Earth Science Series*, Houston.

Namson, J.S., and T.L. Davis, 1988, Seismically active fold and thrust belt in the San Joaquin valley, central California: Geological Society of America Bulletin, v. 100, p. 257-273.

Saleeby, J.B., 1986, C-2: Central California offshore to Colorado Plateau: *Geological Society of America, Centennial Continent/Ocean Transect 10*, 63 pp., scale 1:500,000, 2 sheets.

Somerville, P., and J. Yoshimura, 1990, The influence of critical Moho reflections on strong ground motions recorded in San Francisco and Oakland during the 1989 Loma Prieta earthquake: *Geophysical Research Letters, v. 17*, p. 1203-1206.

Tottingham, D. M., and W. H. K. Lee, 1989, User manual for XDETECT, in W. H. K. Lee, editor, Toolbox for seismic data acquisition, processing, and analysis, *Intern. Assoc. Seism. Phys. Earth Inter. (IASPEI) Software Library Vol. 1*, p. 89-118.

Trehu, A., 1991, Tracing the subducted oceanic crust beneath central California continental margin: Results from ocean bottom seismometers deployed during the 1986 Pacific Gas and Electric EDGE experiment: *Journal of Geophysical Research, v. 96*, p. 6493-6506.

Trehu, A., T. Holt, J. Shi, Y. Nakamura, T. M. Brocher, and M. Moses, 1990, Preliminary results from the 1989 Oregon onshore-offshore seismic imaging experiment: *EOS Transactions of the American Geophysical Union, v. 71*, p. 1588.

Uchupi, E., and K.O. Emery, 1963, The continental slope between San Francisco, California and Cedros Island, Mexico: *Deep-Sea Research, v. 10*, p. 397-447.

U.S. Geological Survey staff, 1990, The Loma Prieta, California, earthquake: An anticipated event: *Science, v. 247*, p. 286-293.

Zoback, M.D., and others, 1987, New evidence on the state of stress of the San Andreas fault system: *Science, v. 238*, p. 1105-1111.